Review Article

Nano Research
2022, 15(5): 4374–4394

ISSN 1998-0124 CN 11-5974/O4
https://doi.org/10.1007/s12274-021-4017-4

State of the art in flexible SERS sensors toward label-free and onsite detection: From design to applications

Liping Xie[1] (✉), Hedele Zeng[1], Jiaxin Zhu[1], Zelin Zhang[1], Hong-bin Sun[3], Wen Xia[1], and Yanan Du[2] (✉)

[1] *College of Medicine and Biological Information Engineering, Northeastern University, Shenyang 110169, China*
[2] *Department of Biomedical Engineering, School of Medicine, Tsinghua University, Beijing 100084, China*
[3] *Department of Chemistry, Northeastern University, Shenyang 110819, China*

Received: 13 October 2021 / **Revised:** 23 November 2021 / **Accepted:** 23 November 2021

ABSTRACT

Surface-enhanced Raman scattering (SERS) as a powerful non-invasive spectroscopic technique has been intensively used in bio/chemical sensing, enabling ultrasensitive detection of various analytes and high specificity with a fingerprint-like characteristic. Flexible SERS sensors conformally adapting to nonplanar surfaces and allowing swab-sampling or *in-situ* detection of analytes, which are not achievable for rigid SERS sensors, greatly meet the demand of onsite and real-time diagnostics. However, the rational design and fabrication of flexible SERS-based sensors for point-of-care diagnostics aiming to simultaneously achieve extremely high sensitivity, stability, and good signal reproducibility remain many challenges. We present a state-of-the-art review of the flexible SERS sensors. Attentions are devoted to engineering plasmonic substrates for improving the performance of flexible SERS devices. Strategies of constructing the flexible SERS sensors toward point-of-care detection are investigated in depth. Advanced algorithms assisting the SERS data process are also presented for intelligently distinguishing the species and contents of analytes. The promising applications of flexible SERS sensors in medical diagnostics, environmental analyses, food safety, and forensic science are displayed. The flexible SERS devices serving as powerful analytical tools shed new light on the *in-situ* and point-of-care detection of real-world analytes in a convenient, facile, and non-destructive manner, and especially are conceivable to serve as next-generation wearable sensors for healthcare.

KEYWORDS

surface-enhanced Raman scattering (SERS), flexible sensor, point of care, swab-sampling, algorithms

1 Introduction

Since the first observation of surface-enhanced Raman scattering (SERS) spectra in 1974 [1], SERS has become a powerful non-invasive spectroscopic technique due to the advantage of high sensitivity at the single-molecule level, arising from the combination of Raman spectroscopy's fingerprint and localized surface plasmon resonances enhanced sensitivity [2]. Raman signals of most molecules are inherently weak and their scattering light intensity is about 10^{-6}–10^{-9} of the incident light intensity due to their small Raman scattering cross-sections, which greatly limits the applications and development of Raman spectra [3]. SERS employs the optical properties of plasmonic nanostructures, resulting in significant Raman signal enhancement of target molecules positioned in proximity to novel plasmonic metal nanostructures [4, 5]. The largest enhancement is typically encountered at narrow interparticle gaps of a highly enhanced electric field usually called hot spots, which yields SERS enhancement factor (EF) of 10^{11} orders of magnitude [6]. SERS contains the native fingerprint vibrational information of the target, which is employed to identify and quantify analytes [7]. The synergy among the extremely high sensitivity provided by plasmonic nanomaterials, the molecular specificity, and the high experimental flexibility of Raman spectroscopy turn SERS into a sensitive, rapid, non-destructive, and powerful analytical technique in medical science [8–11]. SERS exhibits many particular advantages for biochemical analyses. Firstly, SERS is the direct, label-free measurement of analysts compared with fluorescence-based measurement [12]. Besides, SERS can achieve excellent detection sensitivity even down to a single-molecule level as a consequence of significant signal enhancement from plasmonic nanostructures [13]. Moreover, SERS is resistant to photobleaching and photodegradation compared with fluorescence, which is suitable for long-term and real-time monitoring. Notably, the bandwidth of Raman band is significantly narrow and sharp (with a peak width of 1–2 nm), which is 10–100 times narrower than that of fluorescence emission peaks from organic dyes, achieving tremendously increased resolution and multiplexing capabilities [14]. However, there are also some limitations of the SERS technique. Most of the plasmonic substrates are not stable, and easily degrade with time, resulting in decreases in signals. In addition, some substrates are limited to homogeneity and low substrate-to-substrate reproducibility of the SERS signals [10]. It is still challenging to prepare SERS substrates with simultaneous high sensitivity, uniformity, reproducibility, and biocompatibility.

Conventional rigid SERS substrate requires complex extraction of analytes and tedious sample preparation steps before SERS analyses. In contrast, flexible SERS substrates, such as polymer

Address correspondence to Liping Xie, xielp@bmie.neu.edu.cn; Yanan Du, duyanan@tsinghua.edu.cn

films, paper, and cotton, endow new functionalities and provide superior advantages over rigid SERS substrates, largely extending the applications of SERS. Firstly, the high flexibility of the substrates renders them well adaptive to various curved surfaces for efficient Raman spectra collection and *in situ* analyses [15]. It is possible to adopt a swab-sampling strategy for non-destructive detection of analytes from complex real-world surfaces without the intervention of the analyzed system [16]. Secondly, the high transparency of the SERS films makes them promising for *in-situ* detection [17]. The detection signals can be collected from both the front and back sides of the transparent films. Thirdly, the elastic deformation property of the flexible films enables them to achieve tunable SERS substrates with highly active plasmonic nanoarrays [18]. It is possible to enhance SERS signals up to 10 times compared with that of the unstretched one via irreversibly and uniaxially stretching flexible film [19]. Moreover, they are cost-effective, easy-to-operate, and easily integrated into wearable devices owing to the nature of flexible substrates. Currently, flexible SERS sensors are effectively adopted to analyze different types of analytes for on-site testing, including pesticide residues in fruits and vegetables [20], glucose in human tears [21], explosives [22], and microorganisms [23].

Due to the promising applications of flexible SERS sensors, they have received great attention from researchers. Many reviews related to the developments of this field have been reported [15, 24–28]. Li et al. focused mainly on the fabrication and application of transparent and flexible SERS-active films [28]. Hong's group emphasized three categories of recent flexible SERS platforms and their point-of-care diagnostics, including actively tunable SERS, swab-sampling SERS strategy, and *in situ* SERS detection approach [28]. Sun's group mainly summarized the developments in flexible SERS substrates for nondestructive food detection [26]. Liu et al. introduced three categories of flexible SERS platforms and practical applications, including paper-based SERS substrates, polymer-based SERS substrates, and inorganic materials-based SERS substrates [27]. Numerous novel and flexible materials, fabrication methods, and analysis algorithms have emerged in recent years. This review provides a timely summary of recent developments in flexible SERS sensors, highlighting the strategies to fabricate the flexible SERS substrate, the recent improvement of the performance of flexible SERS devices, comprehensive application fields, and analysis algorithms of the SERS data. This review intends to provide the state of the art in flexible SERS-active sensing platforms (Fig. 1). Attentions are devoted to presenting a systematic classification and discussion based on the types of SERS substrates using different materials, including polymer films (polyvinylpyrrolidone (PVP), poly(methyl methacrylate) (PMMA), polyethylene terephthalate (PET), polydimethylsiloxane (PDMS), etc.), hydrogel, sponge, commercial adhesive tape, cellulose filter paper, glass-fiber filter paper, cotton, and natural biomaterials (leaf, petal, insect wing, etc.). Strategies for constructing flexible SERS sensors toward point-of-care detection are investigated in depth. In addition, fabrication methods for flexible SERS substrates and the performance of the SERS platforms are highlighted. The applications of the flexible SERS technique in medical diagnostics, environmental analyses, food safety, and forensic science are summarized. Advanced algorithms assisting SERS data processing for intelligently distinguishing the species and content of analytes are also presented. Finally, we point out the potential problems and challenges, and look forward to the potential solutions for their ultrasensitive sensing applications. The flexible SERS sensors hold intriguing applications in global markets due to their flexibility, non-destructive testing, and sensitivity.

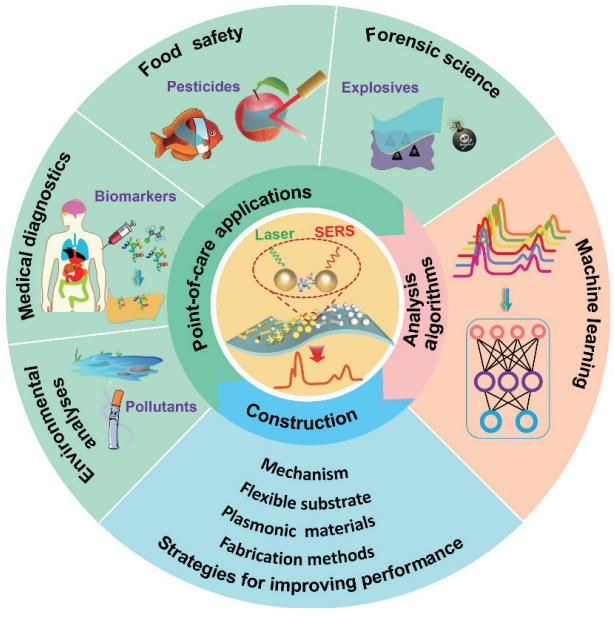

Figure 1 Schematic graph of constructing flexible SERS sensors and their applications.

2 Mechanism of SERS

SERS effect refers to a phenomenon that the intensity of the measured Raman signal of the analyte is enormously enhanced when it is close to certain SERS-active nanostructures [29, 30]. Electromagnetic enhancement (EM) and chemical enhancement (CM) are the widely accepted SERS mechanisms by academics [31]. The EM mechanism dominantly contributes to the enhancement in SERS, resulting in enhancement factors from 4 to 11 orders of magnitude [4]. The local electromagnetic field enhancement originates from the plasmonic properties of SERS-active nanostructures (such as Ag, Au, Cu, and Pt nanostructures). These metals are less prone to inter-band transition because of the relatively larger energy gap between d and s electrons compared with that of transition metals. The energy of the incident light can achieve an efficient localized surface plasmon resonance (LSPR) scattering process, and avoid being converted into heat with an appropriate excitation light wavelength.

As shown in Fig. 2, the incident light-induced electric field drives the conduction band electrons at the interface of metallic nanostructures into collective oscillation. LSPR occurs when the frequency of the incident light matches with the inherent oscillation frequency of electrons in the plasmonic nanostructure, leading to an amplified field [9]. Thus, the Raman scattering cross-section of the analyte at or near the surface of the metal increases by many orders of magnitude [12]. Although EM mechanism plays a dominant role in SERS, CM originating from charge

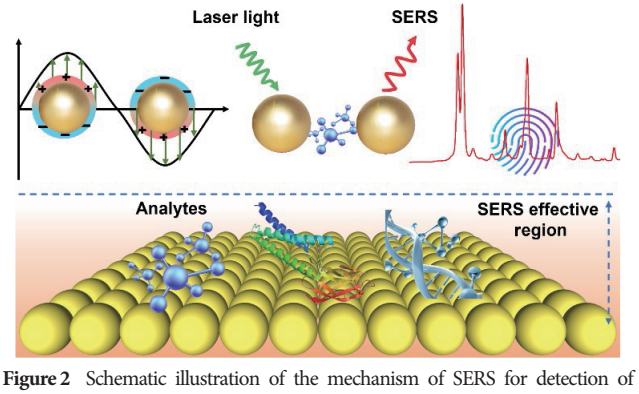

Figure 2 Schematic illustration of the mechanism of SERS for detection of analytes.

transfer between the molecule and the metal surface or semiconductor also has a positive effect [32]. When the analyte is directly adsorbed to the plasmonic metal surface, about 10^2–10^3 times enhancement is contributed by CM due to the increased polarizability of the molecule induced by charge transfer [33, 34]. The localized electromagnetic field decays exponentially from the distance between the molecule and the metal surface. EM is a long-range effect limited by the localized electromagnetic field (within 5 nm), while CM is a short-range effect on the angstrom scale (1–5 Å) with a direct interaction between the analyte and the metallic surface [2, 4, 9]. Surface plasmon resonances induced by incident light localize and concentrate electromagnetic radiation, amplifying the electric fields in the near-field region close to the surface of the plasmonic substrate, thereby leading to extremely large SERS enhancement up to many orders of magnitude. The nanoscale interparticle gaps or sharp regions of plasmonic nanostructures with a dramatically enhanced local electromagnetic field are usually called hot spots, yielding extremely strong SERS signals [2]. Besides, tailoring the plasmonic peak of the metal nanostructure relative to the laser excitation wavelength to achieve resonance is crucial for sensing applications. The measurement under resonance can create a high enhancement factor of the SERS signal [35, 36]. The plasmon peak of the metal nanostructure depends strongly on the size, shape, local dielectric environment, composition, the electron density of metal nanostructure, the effective electron mass, etc. [37]. Hence, the development of SERS substrates with reproducible hot spots to achieve a huge SERS enhancement is highly crucial for sensitive and reliable targets analyses and surface characterization of various materials.

3 Engineering plasmonic substrate

Generally, an ideal SERS-active flexible substrate is expected to possess high-density of hot spots with excellent uniformity, good reproducibility, superior reusability, and low cost. The flexible substrates, plasmonic metal, and fabrication methods contribute to the performance of the flexible SERS sensors. These factors decide plasmonic nanostructures of the substrates and relevant parameters, such as surface homogeneity, inter-particle distance, hot spot density, and further affect macroscopical performance.

3.1 Flexible substrate

Flexible substrate materials have a great influence on exceptional SERS performance, detection, and sampling manners. The flexible materials endow SERS devices with the adaptability of sample collection on non-planar surfaces, portability, flexibility, simplicity, and cost-effectiveness. Table 1 summarizes commonly used flexible substrate materials and lists their advantages and disadvantages. Many polymer materials (e.g., polyethylene terephthalate (PET), polymethyl methacrylate (PMMA), PVP, PVC, PE, PDMS, polyvinylidene fluoride (PVDF), etc.) have been employed as flexible substrates. These materials are flexible, robust, biocompatible, and transparent, allowing SERS sensors to fit non-planar surfaces and conduct *in-situ* detection. These polymers as macroscopic mediators for creating arbitrary purpose-directed nanostructures are suitable for various types of patterning fabrication methods, such as reactive ion etching (RIE) [38, 39], laser patterning [23], nanotransfer printing technique [40], and electron-beam lithography (EBL) [41]. A flexible substrate with uniform surface nanostructure on a large scale can be created by these processing techniques, and thus homogeneous hot spots distribution can be constructed combined with plasmonic metal modification. Due to its legible SERS signals and outstanding optical transparency, a PMMA film with pyramidal structure was hybridized with graphene oxide/Ag nanoparticles as a three-dimensional (3D) flexible SERS substrate [42]. The transparent 3D flexible substrate with pyramidal structure offers large surface area, which is conducive to creating large field enhancement and realizing *in-situ* detection on the curve surface. PDMS, as a class of versatile polymer elastomer, has been widely used in flexible SERS substrates. PDMS owning high mechanical strength can be easily fabricated with various sizes and shapes [43]. Especially, PDMS can be curved or stretched to modulate LSPR and enhance signal intensity [44, 45]. However, the background signal of PDMS is strong and should be measured initially to make sure it doesn't overlap with the SERS signal of the target [46]. Hydrogel is a network of hydrophilic polymer chains and doesn't have strong mechanical strength. It suffers from low stability due to its sensitivity to the external environment (e.g., pH, temperature) and uncontrollable structure change during dehydration and rehydration [47, 48]. Nevertheless, some hydrogels have phase transition properties and can respond to stimuli, endowing the device with good selectivity [49, 50]. Sponge as a new type of SERS substrate possesses high porosity, which can extract liquid samples efficiently [51, 52]. However, the pores of sponges with random distribution may lead to limited reproducibility [53]. Some recent

Table 1 Various flexible materials severed as SERS substrates

Flexible substrate	Advantage	Disadvantage	Ref.
Polymer films (PVP, PMMA, PET, PDMS, etc.)	Easy to be obtained, low cost, easy functionalization, transparency	Cannot withstand very high temperature, low strength to size ratio of polymer	[23, 38, 39, 44, 45, 70]
Hydrogel	Stimuli-responsive, sensing capability, user-friendly	Low mechanical strength, easy to lose water, low stability	[47–50, 71]
Sponge	High water absorption ability, no need of any complicated extraction procedures, suitable for both solid surface and liquid sample	Low reproducibility	[51–53]
Commercial adhesive tape	Enable direct sample collection, transparent, low cost, versatile applicability, easy to be obtained	Unwanted background signals, plasmonic metal detachment	[22, 55, 72]
Cellulose filter paper	Natural wrinkles, fibril structures, and wicking property, biodegradable, low cost and no-interference with Raman signal, high surface area, easy to be obtained, easy functionalization	Low mechanical strength, metallic nanoparticles are not easily evenly distributed	[73–75]
Nanocellulose	Controllable nanostructure, relatively high transparency, good surface uniformity and homogeneity, biodegradable, no interference with Raman signal	Low mechanical strength	[66, 76–79]
Glass-fiber filter paper	Tolerant to biochemicals or chemicals, wicking property, thermostability, corrosion resistance, and low cost	Complicated functionalized process	[69, 80–82]
Cotton	Biodegradable, no interference with Raman signal, low cost, high mechanical strength, ability to be woven into wearable fabrics	Uneven surface	[68, 83–86]
Natural biomaterials (leaf, petal, insect wing, etc.)	Biodegradable, low cost, easy fabrication, hydrophobicity	Difficult for mass-produced, short shelf time	[87–92]

literatures show that transparent adhesive tape is a type of promising substrate material for non-invasive sample collection and measurement [54]. The specific "paste and peel off" approach of transparent tape does not need a wet surface for sample extraction, which avoids unwilling changes of the sample characteristics [22, 55] and performs perfectly on different surfaces [56]. Nevertheless, noise signals caused by the interference from the sticky layer and incomplete collection are still noticed in actual use [57, 58].

Paper is commonly used as a flexible substrate for SERS sensing, due to its ubiquity, adaptability, and affordability. Cellulose paper has been proved as a remarkable substrate material because of its low cost, inherent capillary effect, biocompatibility, biodegradability, and minimal SERS interference [59–61]. The heterogeneous nanostructure of paper is beneficial to improve sensitivity by forming 3D hot spots [62–64]. Paper with appropriately low porosity facilitates uniform distribution of analytes on the detection substrate, thus avoiding forming a "coffee ring" and achieving good uniformity of SERS signals [65]. Compared with cellulose paper, nanocellulose paper has well controllable structure and large surface area [66, 67]. Ordered structure, uniform nanopores, and homogenous chemical group endow nanocellulose paper with uniform metal nanoparticle distribution, further realizing its outstanding Raman signal enhancement and reproducibility [64, 67]. Cotton is a rising star as a flexible substrate due to its little SERS interference signal as well as the robustness of cotton fabrics [62, 68]. Plasmonic cotton fabric can be woven into clothes and conduct wearable flexible SERS substrate. In comparison with paper, the lower absorbency and more compact size of thread reduce the need of reagent as well [68]. Glass-fiber paper as a special fiber material is known for its chemical inertness, which has a tolerance for complex circumstances [69]. However, glass-fiber paper inevitably requires complex functionalization processes.

Natural biomaterials have attracted extensive interest from SERS researchers in recent years. Their excellent natural 3D nanostructures with high homogeneity have been used as SERS substrate after being modified with plasmon nanoparticles, thereby greatly simplifying the substrate fabrication process [87]. Moreover, the super-hydrophobicity of some biomaterials also promotes the Raman signal enhancement. Because of the surface tension, the droplet will maintain a spherical shape and concentrate solutes during evaporation [93, 94]. Up to now, natural biomaterials including leaf [49, 87, 88], flower petal [93], eggshell membrane [89], and insect wing [90–92] have been studied. This kind of material does not need sophisticated micro-nano fabrication [91], and their natural 3D nanostructures with high homogeneity facilitate the generation of abundant optical hot spots, thus improving SERS sensitivity and reproductivity synchronously [92]. Nevertheless, some limits of natural biomaterials in preservation and acquisition should be noticed. Some substrates, such as petals and leaves are easy to dry and degenerate, which have limited shelf life. Other animal-derived materials like dragonfly wings and butterfly wings are cheap, but they are difficult to be mass-produced.

3.2 Engineering hot spots

3.2.1 *Selection of plasmonic materials for SERS substrates*

The shape of plasmonic nanoparticles (NPs), such as sphere [95], core–shell nanostructure [96], nano flowers [97], nano stars [98], and nano dendrites [99], significantly affects the density of hot pots. SERS signals enhanced by plasmonic nanocomposites with sharp structures are highly stronger than those enhanced by sphere nanoparticles. Recently, 3D hierarchical plasmonic arrays have already drawn a lot of attention, because external curved regions and internal nanogaps present complicated multiscale coupling conditions, endowing the metallic arrays with a large number of hot spots and the capability of capturing analyte molecules [100, 101]. The enhancement mechanism of noble metal is mainly based on electromagnetic mechanism (EM) [102]. Their outstanding surface plasmonic resonance (SPR) contributes to dipole moment increment, thus enhancing Raman scattering intensity [103]. Theoretically, AgNPs exhibit ultrahigh SERS signal EF and enable the ultrasensitive detection of single molecules due to their high surface free energies [13, 104]. However, Ag NPs tend to be oxidized after long-term storage, which significantly affects the stability of SERS substrate [105, 106]. While Au NPs are more stable and possess good SERS performance. It is common to use Au coupled with Ag to form stabilized nanocomposites for promoting SERS enhancement effect through strong electromagnetic coupling [102]. Nevertheless, the high cost of Au makes it is not an economical choice for flexible SERS devices [107]. Besides, the high oscillation damping of Au causes that the electrons in Au are not as active as those in Ag, resulting in a little lower EF [108]. Cu is expected to be utilized as a substitution of expensive Au and Ag in light of its low cost and abundance [109, 110]. Nevertheless, the insignificant SERS effects limit its wide applications. Relative high EF can be achieved by controlling the nanostructure of Cu [111] or hybridizing with high SERS-active noble metal. Highly ordered Ag/Cu hybrid nanostructure arrays exhibit EF even up to 1.0×10^{10} [112], which combines the advantages of both Ag and Cu.

Semiconductor materials are known for their high SERS reproducibility and uniformity [113]. Compared with metal nanostructures, highly controllable nanostructure parameters (e.g., the exciton Bohr radius, doping type, band structure, chemical stability, geometry, and crystallinity) are also favorable in SERS substrates [114]. However, semiconductors usually exhibit relatively lower EF (10^3–10^5) compared with metal materials [32]. SERS enhancement of semiconductors is believed to mainly rely on the chemical mechanism (CM) [115, 116] via photo-induced charge transfer processes between the adsorbed molecule and the semiconductors substrate. Carbon-based nanomaterials, such as carbon nanotube and graphene, are outstanding and remarkable materials among recent semiconductors for SERS. SERS usually suffers from strong fluorescent interference. Carbon-based nanomaterials are sufficient to quench the photoluminescence of fluorescent dyes and provide a clean SERS spectrum [116]. Graphene is a two-dimensional single-layer material composed of hexagonally placed carbon atoms with sp^2 bonding. A strong π–π stacking between the graphene (or its derivative) and specific molecules contributes to improving sensitivity and selectivity [117, 118]. Graphene oxide (GO), a derivative of graphene with oxygen-rich functional groups, is also employed as SERS sensitive layer due to charge transfer between analytes and GO [119]. Additionally, target molecules with aromatic structures are favorable to attach onto graphene surfaces by π–π stacking, which facilitates SERS performance by enriching the number of targets on SERS substrates. Recent studies were dedicated to combining semiconductors and metal NPs in a stratified structure and taking advantage of both EM and CM [116, 120–122]. Several studies have explored the combination of graphene with Ag or Au NPs to improve the SERS performance [123]. These hybrid particle systems achieve an increase of the SERS signal due to the synergism between the EM effect originating from metal nanostructure and the CM effect deriving from the graphene [124].

3.2.2 *Fabrication methods of flexible SERS substrate*

Flexible SERS substrates are usually composed of plasmonic

nanostructures supported by a flexible film or fibers. SERS substrate possessing well-controlled plasmonic features is pivotal for obtaining a highly sensitive and reproducible SERS sensor. Various methods have been developed for the fabrication of nanostructured SERS substrates, such as *in-situ* synthesis, dip coating, magnetron sputtering, electrodeposition, drop casting, inkjet printing, gravure printing, self-assembly, and nanoimprint (Table 2).

In-situ synthesis is a classical method for metallic SERS substrate fabrication. Plasmonic metal NPs or metallic coating are synthesized directly on the surface of the flexible supports by oxidation–reduction reaction [28, 125]. The *in-situ* synthesis is favorable to achieve homogeneous NPs distribution and avoid nanoparticle aggregation which significantly affects reproducibility [126]. Fortuni et al. took advantage of *in-situ* synthesis approach and successfully obtained flower-like Ag@Au-shell NPs on PDMS sheet [127]. Ascorbic acid (AA), sodium citrate (Cit), and $AgNO_3$ solution were applied on PDMS surface in turn. Thus, Ag_x-Cit complexes that resulted from the chelating ability of Cit could be formed, further inducing the flower-like morphology of AgNPs. Then, AgNPs coated PDMS film were immersed in growth solution with AA, NaOH, and $HAuCl_4$ solution for 1 h to form Au shell while maintaining the flower-like feature. The SERS sensor fabricated by the proposed method presented up to 1.07×10^5 SERS EF and showed slight signal change after storage of one week in air due to oxidation resistivity of the Au shell. Moreover, the same group also took the advantage of the reducing property of PDMS and proposed a facile one-step *in-situ* synthesis protocol [125]. Growth solutions containing Au ion, Cit, and hydroxylammonium chloride were mixed and simply dropped on a newly polymerized PDMS surface with residual of curing agent (Si-H), resulting in gold NPs with star shape. The gold nanostars coated PDMS sheet were then used in the measurements of thiabendazole and realized down to a limit of detection (LOD) of 10^{-5} M. The interactions between substrate and metal particles, types of the surfactant, and weak reducing agents are essential to the formation of homogeneous and monodisperse metal NPs layer on the substrate. Chen et al. developed flexible plasmonic fibers by *in-situ* growth of AuNPs on the high-curvature surface of PVDF nanofibers [128]. As shown in Fig. 3(a), the flexible membrane composed of PVDF fibers was modified with Au seeds by employing electrostatic interaction. Then, the coordinating ligand of KI was applied to form a stable AuI_4^- complex with $AuCl^-$ in the growth solution, which could restrain the self-nucleation of Au. *In-situ* growth of AuNPs on the surface of PVDF fibers was initiated by the presence of PVDF@Au seeds, forming in large-scale homogeneous hot spots generated by the coupling of adjacent AuNPs in the porous 3D morphology of fiber membrane. A prominent SERS signal was acquired for the detection of bacteria, because of a close spatial distance between 3D space of hot spots and the surface of bacteria.

Physical vapor deposition (PVD), such as magnetron sputtering and e-beam evaporation, is a mature industrially viable technique that allows rapid fabrication of thin films and surface coatings. The PVD approach is based on heating-induced evaporation or plasma-based ion bombardment on a source substrate. Preliminary materials are sputtered or evaporated under vacuum conditions, finally deposit on target substrate via condensation. SERS substrates with uniform plasmonic nanostructure distribution and highly controllable film thickness ensure high reproducibility of SERS signals [135, 136]. Gao et al. fabricated a flexible SERS-active substrate by magnetron sputtering [85]. As shown in Fig. 3(b), Ag film was deposited on a large area of cotton fabrics to construct a SERS sensor, which displays a strong, reproducible, and stable enhancement of Raman signal. The PVD method is widely used for large-scale and time-saving deposition of thin plasmonic films on different types of materials [23, 82, 85]. Zhang et al. adopted PVD to metalize a sheet with tapered pillar patterns for SERS substrate fabrication [137]. Au layers with different thicknesses (15, 30, 45, and 60 nm) were uniformly coated on irregular nanostructure surfaces by adjusting the ion sputtering time. However, PVD method suffers from expensive instruments and needs to be operated by well-trained operators. Interfacial self-assembly is a simple, low-cost fabrication method for flexible SERS substrate. Generally, self-assembly of plasmonic NPs occurs at the interface of an immiscible two-phase system. The NPs suspended in an aqueous solution would rise and orderly assemble at the diphase interface during the volatilization process [138]. The assembly plasmonic NP layer shows a close and uniform pattern [139], which can be transferred [105, 131, 140] or embedded in a flexible substrate [141], thus forming SERS substrate with high performance. Wu et al. have demonstrated a one-step self-assembly method to fabricate AuNPs/PVC films for *in situ* multi-pesticide residues measurement (Fig. 3(c)) [141]. PVC cyclohexanone solution was added to the top of AuNPs solution. When the cyclohexanone evaporated, AuNPs would rise to the cyclohexanone/water interface and be half-embedded at newly formed PVC film. The PVC film played two roles in the

Table 2 Methods for fabrication of flexible SERS-active substrate

Fabrication method	Substrate material	Plasmonic metal	Enhancement factor	Analytes and limit of detection	Ref.
In-situ synthesis	PI[a]	Ag@Au NPs	1.0×10^7	10^{-9} M (BPE[b])	[129]
Electrodeposition	PET[c] film	AgNPs	3×10^7	10^{-13} M (TNT[d])	[39]
Magnetron sputtering	Cicada wing	Cu@Ag core–shell NP	3.1369×10^5	10^{-11} M (4-ATP[e]); 10^{-10} M (CV[f])	[107]
In-situ self-assembly	amPEN[g]	AgNPs	10^8	10^{-10} M (chlorpyrifos)	[130]
Self-assembly and transfer	PDMS[h]	AuNPs	9.16×10^7	10^{-12} M (CV[f]); 10^{-10} M (MG[i]);	[131]
Dip-coating	PDMS[h]	AgNPs	9.2×10^9	8×10^{-12} M (R6G[j])	[132]
Drop casting	Aluminum foil	AgNPs	1.03×10^8	100 cfu·ml^{-1} (*S. aureus*[k]) 1,000 cfu·ml^{-1} (*E. coli*[l])	[133]
Inkjet printing	Chromatographic paper	Au nanospheres	2.0×10^6	10^{-11} M (thiram)	[95]
Incorporation	Chitosan film	AuNPs	1.4×10^7	1.5 mg·kg^{-1} (melamine) 0.001 mg·kg^{-1} (thiamethoxam)	[134]
Nanoimprint and sputtering	PDMS film	AuNPs	2.24×10^7	10^{-11} M (R6G)	[135]

[a]PI: polyimide. [b]BPE: 2-di-(4-pyridyl)-ethylene. [c]PET: polyethylene terephthalate. [d]TNT: 2,4,6-trinitrotoluene. [e]4-ATP: 4-aminothiophenol. [f]CV: crystal violet. [g]amPEN: amphiphilic polyarylene ether nitrile. [h]PDMS: polydimethylsiloxane. [i]MG: malachite green. [j]R6G: rhodamine 6G. [k]*S. aureus*: *Staphylococcus aureus*. [l]*E. coli*: *Escherichia coli*.

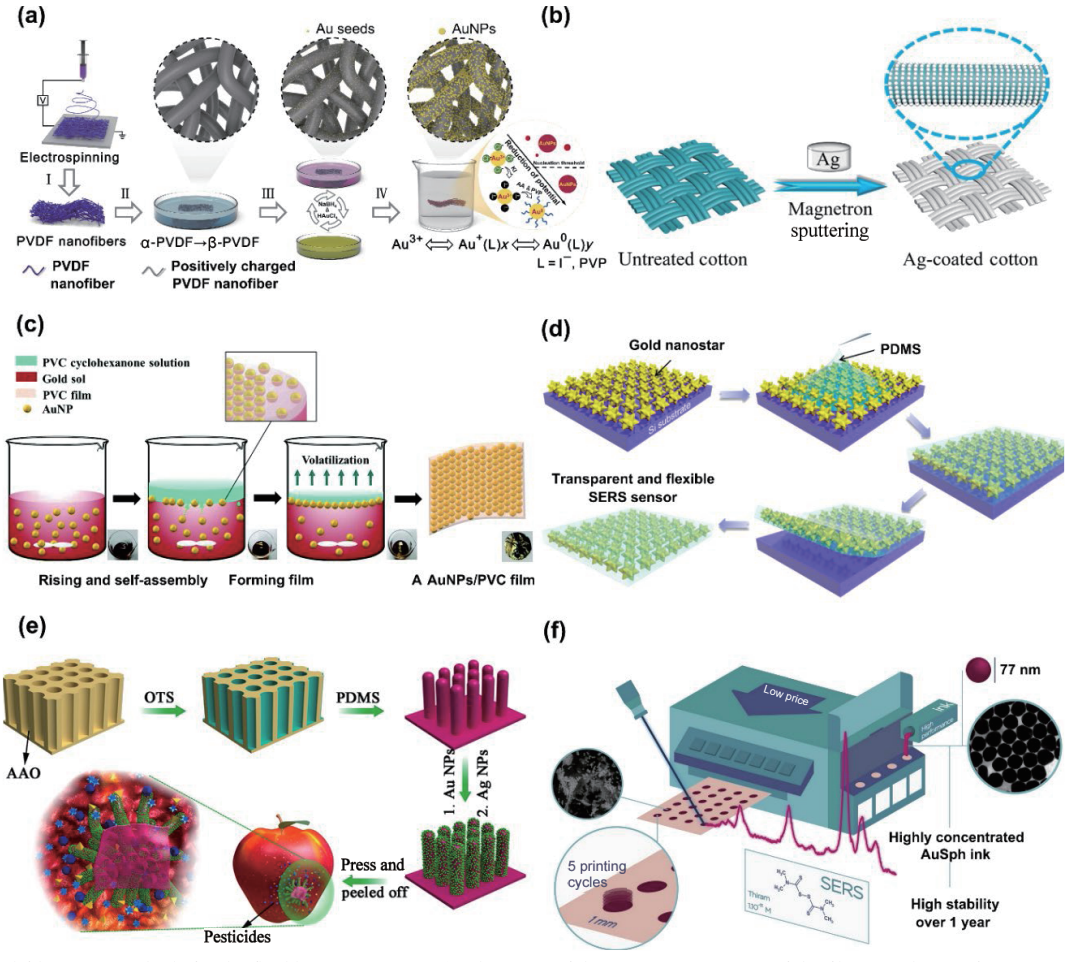

Figure 3 Typical fabrication methods for the flexible SERS sensors. (a) Schematics of the preparation process of the fiber membrane of PVDF@Au nanofiber. (I) PVDF nanofiber membrane produced by electrospinning. (II) The surface charge of PVDF fibers was changed by incubation with ethanol. (III) The surface of PVDF fibers was deposited with Au seeds by repetitive ionic layer adsorption reaction. (IV) PVDF@Au nanofiber was formed by introducing PVDF@Au seeds. Reproduced with permission from Ref. [128], © Tsinghua University Press and Springer-Verlag GmbH Germany, part of Springer Nature 2021. (b) Schematic of fabricating superhydrophobic Ag coated cotton SERS substrate. Reproduced with permission from Ref. [85], © Elsevier B.V. 2019. (c) Schematic of a fabrication process of a AuNPs/PVC film, reproduced with permission from Ref. [141], © Royal Society of Chemistry 2019. (d) Schematic diagram shows that self-assembled gold nanostar arrays are transferred into PDMS to construct flexible SERS sensor. Reproduced with permission from Ref. [98], © American Chemical Society 2017. (e) Schematic illustration of fabricating gecko-like flexible SERS sensor. Reproduced with permission from Ref. [20], © American Chemical Society 2017. (f) A commercial inkjet printer for inkjet-printing method. Reproduced with permission from Ref. [95], © Elsevier B.V. 2020.

one-step fabrication process, both inducing the interfacial self-assembly of AuNPs and fixing the AuNPs in the polymer matrix to form a flexible SERS-active sensor. The sensor exhibited outstanding sensitivity with 3.7×10^6 EF and presented remarkable reproducibility and stability after 1 h ultrasound treatment and filter paper rubbing. Interfacial self-assembly is usually combined with other strategies, such as transfer strategy, allowing researchers to design complex plasmonic nanostructure and increase hot spot numbers. Zhang et al. demonstrated a SERS-based film through the conventional self-assembly and transfer strategy for pesticide detection [131]. AuNPs were firstly self-assembled at air–water surface and then PDMS film that patterned with ordered micro-hemisphere array was applied on the AuNPs surface. AuNPs were transferred and anchored onto PDMS film, endowing the film with high SERS sensitivity. Park et al. fabricated a transparent and flexible SERS sensor based on self-assembly and transfer strategies [98]. As shown in Fig. 3(d), gold nanostars (GNS) modified with positive charge were uniformly self-assembled on a substrate with high density by a dip-coating process. A liquid PDMS mixture containing prepolymer and curing agent was poured onto the substrate with the assembled GNS monolayers. After curing, a flexible PDMS thin-film embedded with the GNS arrays was achieved, which exhibits an enormous SERS EF (~ 1.9×10^8) because of the plasmon couplings between GNS and Ag film, and high stability after mechanical deformation of 100 cycles. High robustness and stability can be achieved, due to the firm incorporation between the nanoparticles and the substrate material.

Drop casting and dip coating are two typical approaches that directly load synthesized NPs colloid onto a substrate for constructing SERS plasmonic device. It is believed that the significant parameters, such as particle diameters, shapes, and chemical characteristics, can be well controlled in advance [142]. Drop casting or dip coating combined with patterning strategies, such as nanoimprint pattering, can improve the number of hot spots. PDMS film with gecko toe-pads-like multiscale structure was constructed by a highly ordered anode aluminum oxide (AAO) [20]. As shown in Fig. 3(e), the PDMS nanotentacle array was modified with Au NPs and Ag NPs by dip coating. The flexible gecko-inspired-SERS sensor exhibited strong adhesive force and large contact area toward almost any surface, which facilitates efficient target sampling from uneven surfaces. In addition, gecko-nanostructure produced abundant hot spots and thus ensured considerable enhancement of SERS signals. The drop casting and dip coating are particularly suitable for fiber-based SERS substrate [133, 143]. The capillary tubes within the substrate offer it with wicking property, which facilitates rapid deposition of NPs without extra pressure. Nevertheless, the coffee-ring effect

should be noticed. Suspended NPs are likely to aggregate at the edge of the liquid phase and form stochastically deposited clusters along with evaporation, which causes unrepeatable SERS measurements [144, 145]. In addition, the prepared NPs are faced with a high risk of particle aggregation due to the change of environmental conditions during the decorating step. Some easy and simple methods, such as screen printing [146], and gravure printing [70] are also utilized in low-cost SERS substrate fabrication. Plasmonic NPs solution also can be automatically printed onto a substrate to realize high-throughput detection. Many thin and flexible substrates (such as paper, thin polymer films) can be processed by a commercial inkjet printer. The inject printing method is easy-to-use, inexpensive, and can produce large-scale substrates in a short time [147, 148]. The plasmonic nanostructures with high-throughput arrays can be formed by deposition of metal NPs on the surface of a flexible substrate as well as using template-assisted techniques or hydrophobic modification, which can control the spreading of aqueous analytes, thereby improving the SERS response and realizing a high-throughput detection. By using the inkjet-printed technique, Godoy et al. produced a hydrophobic paper-based ultrasensitive SERS sensor (Fig. 3(f)) [95]. Chromatographic paper was initially immersed in (2-dodecen-1-yl)-succinic anhydride hexanol solution and baked to endow the surface with hydrophobicity. The hydrophobic patterned paper was modified with 77 nm Au nanospheres (AuSphs) by a commercial printer. Because of the hydrophobicity, printed AuSphs and analytes would be concentrated upon evaporation, thereby promoting the SERS sensitivity. This device reached a LOD of 10^{-11} M in both crystal violet and thiram measurements. The cost was only 0.01 dollar per detection spot. Inkjet-printing method is suitable for low-cost SERS sensor fabrication in resource-limited areas, but the NPs of the ink are easy to aggregate, which leads to nozzle blockage. It is necessary to fabricate stable NPs ink reasonably.

Directly incorporating metal NPs within the substrate material can easily and quickly produce a flexible SERS substrate. Metal NPs embedded in hybrid sponges have been fabricated to measure liquid samples [51, 52]. Similarly, Sykam et al. added AgNPs into graphite powder and compressed it to form a flexible sheet as a SERS platform [149]. The fabricated SERS sensor achieved a remarkable R6G detection limit down to 10^{-12} mol·L^{-1}. Plasmonic NPs embedded in flexible substrate provides a firm integration between NPs and the substrate, which enhances the stability of the sensor. Fu et al. recently created a sensitive SERS substrate biosynthesized by an aqueous chitosan-alkali/urea solution system [134]. The chitosan nanofibrils decorated with well-distributed Au NPs were self-assembled and formed SERS substrate with 3D porous geometry based on the unique inclusion channel structure formed in an aqueous alkali/urea solvent. The sensor achieved EF up to 10^7 and spot-to-spot reproducibility as low as 5.66% relative standard deviation for detection of 4-mercaptobenzoic acid. Moreover, the characteristic amino groups of chitosan chains endowed this substrate with promising charge selectivity for counter-charged analytes.

4 Strategies for improving SERS performance

SERS substrate with high sensitivity, stability, and good signal reproducibility is preferable for SERS-based detection. Many efforts have been devoted to optimizing the performance of flexible SERS sensors through the rational design and development of structurally uniform substrates.

4.1 Sensitivity

Sensitivity is one of the most important properties for SERS-based trace applications. Significant progress has been made in improving the sensitivity of the substrate. It can be realized by directly increasing the surface roughness, thus increasing the density of optical hot spots [150]. Local electromagnetic field, the dominant enhancement mechanism of Raman signal, can be promoted within rough surfaces with large surface areas and close intervals. Xu et al. compared the LOD of SERS-based melamine measurements using different plasmonic nanostructures, which proved that densely arranged sliver nanostructures with higher surface roughness had the potential to achieve higher sensitivity [151]. Nowicka et al. demonstrated that PET/indium tin oxide/Ag substrate achieved 100 times higher SERS signal intensity after surface dielectric barrier discharge treatment [136]. The elemental compositions and sharp morphologies of plasmonic NPs are also critical for achieving ultrasensitive detection [125]. With the fast development of nanotechnology, complex nanostructures with ordered architectures play a significant role in improving the sensitivity of SERS substrate [152]. The vertically aligned structure is popular in recent studies, which can be fabricated by top-down techniques (e.g., photolithographic, etching) and bottom-up methods (e.g., screen printing, physical vapor deposition). The vertically aligned nanostructures combined with plasmonic NPs with tuneable properties significantly increase the density of hot spots and surface area, which are desirable for SERS-based trace level detection. Cai et al. took the advantage of nanoimprint technique to replicate delicate hierarchical patterns of natural bio-template of diatom frustules onto PDMS film [135]. Au NPs were deposited on the PDMS film with the regular and periodic nanostructures by sputtering, achieving high sensitivity (EF: ~ 2.24 × 10^7) and good Raman signal reproducibility. The nanostructure of flexible SERS active substrate significantly contributes to the enhancement of SERS signals. Worm-like Au nanostructures on polyethylene terephthalate were achieved by Ar plasma etching and Au evaporation, exhibiting high SERS EF (~ 1.2 × 10^8) and trace level detection sensitivity (10^{-9} M R6G) [153]. Guo et al. fabricated uniform 3D nanopillar arrays on a flexible Nafion sheet using colloidal lithograph and plasma etching [154]. Polystyrene (PS) microspheres in an aqueous solution firstly formed a monolayer via self-assembly, which was then transferred on a Nafion surface as the mask of subsequent oxygen plasma etching. Then, a vertical nanopillar substrate with high reproducibility and tunability was obtained by plasma etching. The morphology of the surface nanostructure could be changed by adjusting the diameter of PS microspheres. The substrate exhibited LOD of 10^{-11} and 10^{-10} M for R6G and MG measurements respectively after being coated with Ag layer. Designing 3D plasmonic complex nanostructures with more than two composites contributes to improving SERS performance. Wei et al. provided a flexible and robust SERS sensor composed of a silver NPs@nanowire network embedded in PDMS [155]. The unique network structure contributed to high sensitivity (EF of 3.4 × 10^9) and extremely low detection limit (10^{-11} M for malachite green), which is resulted from rich plasmonic hot spots via enhancing the electromagnetic field of AgNPs surrounding AgNWs.

The overlap plasma electromagnetic field induced by the electromagnetic coupling of two plasmonic composites can greatly increase sensitivity [158]. Gao. et al. reported a novel SERS substrate based on the coupling between Au coated wrinkled nanocones and AgNPs for highly sensitive TNT detection (Fig. 4(a)) [39]. 4-ATP was initially decorated on both AgNPs and Au modified nanocone. The Meisenheimer complex formed by target TNT and the 4-ATP made AgNPs close enough to the substrate, generating strong coupling of electromagnetic fields. The LOD of the sensor for TNT analysis was as low as 10^{-13} mol·L^{-1}, and an excellent linear response from 10^{-8} to 10^{-13}

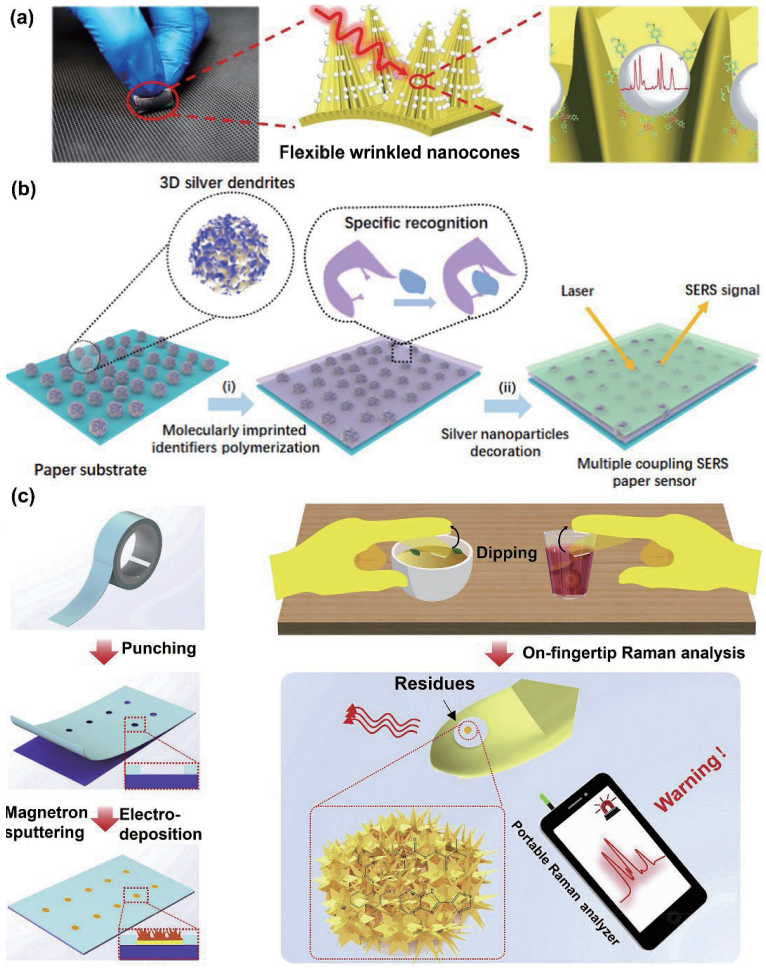

Figure 4 Strategies of improving the sensitivity of the flexible SERS sensors. (a) Illustrations for flexible wrinkled nanocones. Reproduced with permission from Ref. [39], © Elsevier B.V. 2020. (b) Schematic of the construction of multiple EM coupling SERS paper sensor for pesticides detection. Reproduced with permission from Ref. [156], © American Chemical Society 2020. (c) Schematic illustration showing the fabrication processes of tape-based SERS sensors toward on-hand detection of food contaminants by a portable Raman analyzer. Reproduced with permission from Ref. [157], © Elsevier B.V. 2020.

mol·L^{-1} was achieved. Zhao et al. initially synthesized dendrite-like 3D silver materials on a paper substrate (Fig. 4(b)) [156]. The porous feature of paper material endowed the device with largely accessible surface area for plasmonic nanostructures growth and sample loading. AgNPs were subsequently decorated on the top after targets were applied to the silver nanodendrites modified paper substrate. The sandwich-like 3D hybrid nanostructure conducted multistage SERS enhancement and achieved a detection limit of 0.02811 ng·mL^{-1} for imidacloprid detection.

The concentration of analytes on a modified surface is another important way to promote sensitivity. Liquid droplet on the hydrophobic surface keeps a sphere-like shape and small contact area, which makes analytes to densely deposit and concentrate *in situ* after evaporation [93, 159]. The concentration process makes it possible to screen trace analytes and greatly decreases the detection limit. Nevertheless, long evaporation time also limits its feasibility in rapid testing [160]. Moreover, sessile droplets easily roll on a slippery hydrophobic surface [161]. He et al. proposed a tape-based wearable SERS sensor with a hydrophobic–hydrophilic pattern to detect food contaminants, including Sudan-1, thiram, and thiabendazole (Fig. 4(c)) [157]. The commercial double-sided conductive tape was firstly physically punched to generate microwells as a protective layer. Gold-coated conductive tape was formed by mask-assisted sputtering and electrochemical deposition. High capillary force among the hydrophilic patterned microwell enables rapidly sampling analytes solution automatically. After evaporation, SERS signals were measured by a portable Raman analyzer for sensitive on-site screening of different residual pesticides.

4.2 Specificity

SERS signal features highly depend on the structure of the target molecule, which enables both qualitative and quantitative analysis. Nevertheless, noises and signals of other non-target analytes significantly affect the accuracy and effectiveness of complex biofluid measurements [162, 163]. To realize quantitative SERS detection, it is essential and worthwhile to improve both specificity and sensitivity via substrate design and fabrication. Capturing of analyte molecules, both chemical and physical, are usually adopted to enhance the specificity of sensors.

Porous flexible substrate like a filter can effectively filter out interferences of uninterested macromolecules. Because of the adjustable well-defined nanostructure, hydrogel [71] and cellulose [164] are noticed as potential materials for forming filter structures. Hu et al. proposed an Au-decorated cellulose flexible platform for *in-situ* monitoring [165]. The hierarchical pore structure conducted by cellulose chains can prevent macromolecules from contacting with SERS-active AuNPs and benefit practical small molecule detection. Molecular recognition based on the noncovalent bonding interactions, such as hydrogen bonds, ionic bonds, van der Waals forces, and hydrophobic effect, is commonly employed to anchor the molecules at the SERS-active surface. Aromatic molecules, such as serum bilirubin, polycyclic aromatic hydrocarbons, and DNA, could be captured and enriched by graphene materials, through π–π interaction [117, 166, 167]. In addition, self-assembled monolayers (SAMs) were

often employed to modify the substrate as adsorbates for small molecule enrichment. As an instance, (1-mercaptoundeca-11-yl)-tri(ethylene glycol) was used as the self-assembled monolayers on a Ag surface to pre-concentrate glucose within the 0–4 nm thick region of the enhanced electromagnetic field [168].

Affinity ligands are usually grafted onto plasmonic surface to capture and confine the targets close to the surface of SERS substrate for the enhancement of specificity and sensitivity [169–172], including chemical ligands, antibodies, enzymes, aptamers, and molecularly imprinted polymers (MIPs) (Fig. 5). The surface of SERS substrate containing or being modified with specific chemical ligands can selectively capture targets. Fan et al. took advantage of the inherent amino groups on gel pad surface to selectively capture 2,2′,4,4′,6,6′-hexanitrostilbene (HNS) through forming a specific Meisenheimer-alike complex [173]. Reokrungruang et al. conjugated magnetic nanoparticles with antibodies and used them to enrich target cancer cells [174]. The captured cancer cells were transferred to a AuNPs-embedded plasmonic paper, which provided both support and dense hot spots, achieving a recognition accuracy of 98% for cancerous cells screening. Blanco-Covián et al. integrated SERS technique with traditional lateral flow immunoassay devices, realizing a LOD as low as 1 pg·mL^{-1} for pneumolysin, a significant biomarker of pneumonia [175]. Pneumolysin was captured by the 1st antibody on the test line. The tags, Au@Ag core Covián shell NPs grafted with Raman reporter Rhodamine B and 2nd antibody, would be recognized and captured by the 1st antibody. Therefore, SERS signal intensity of Rhodamine B indicated the concentration of pneumolysin. The sandwich immunoassay-based SERS technology provides highly sensitive quantitative detection of multiplex biomarkers in complex body fluids. Some disease-related biomarkers have been identified based on the specific interaction between antibody and antigen. For example, the highly sensitive and quantitative detection of acute myocardial infarction biomarkers in human serum was achieved by using immunoassay-based SERS technology [176]. Similarly, inflammation biomarkers from serum were sensitively detected using antibody functionalized Fe_3O_4@Au magnetic nanoparticles, which can quickly capture and enrich the target infection biomarkers [177]. However, the high cost of specific antibodies and their stability in long-time storage limits their accessibility in resource-limited regions [178]. Aptamer is a short single-stranded nucleic acid that owns high specificity to targets from molecules to entire cells, obtained by systematic evolution of ligands by exponential enrichment (SELEX) [179]. Due to its thermal stability, mass-production property, cost-effectiveness, and high affinity to a specific molecule, aptamer has become a good candidate for developing target-specific biological sensors [180–182]. Zhu et al. developed an aptamer modified SERS sensor for the detection of *S. aureus* [183]. Thiol-terminal aptamers conjugated AuNPs were fixed on PDMS to capture *S. aureus*. Then, signal probes composed of aptamer modified Au@Ag core–shell nanoflowers were applied to form a sandwich-like structure. The aptasensor presented a LOD of 1×10^3 cfu·mL^{-1} with a recovery rate between 92.5% and 110% for target *S. aureus* detection. By integrating aptamer enzymes and Raman reporter Rhodamine B (RhB), He et al. proposed a stimuli-responsive hydrogel sheet that can be used to trace UO_2^{2+} ions among aquatic products [50]. The target UO_2^{2+} appeared in the sample would activate the specific enzymatic cleavage reaction, and then, RhB trapped within the DNA-hydrogel composite was released. The released RhB induced a strong SERS signal. Recently, many efforts have been devoted to developing molecular imprinting polymer (MIP), a novel artificial antibody mimic [156, 184]. Generally, monomers mix with template molecules and form a pre-polymerization complex via either covalent or non-covalent interaction with templates [185, 186]. The template molecules are removed after polymerization, leaving complementary 3D cavities on the polymer surface, which endows MIP with good selectivity. The polymeric material resists harsh environments, possesses a long shelf life, and preserves an economic preference compared with conventional recognizers. Therefore, the MIP technique has gained a great deal of interests in biomedical detection and has been utilized in SERS-based devices for *in situ* detection [156, 187, 188]. Liu et al. synthesized a MIP membrane and integrated it with AgNPs coated paper to detect tartrazine in snacks [158]. Because of the specific stereochemical structure of MIP membrane, other molecules in the sample solution would be washed away, and tartrazine molecules were left on its surface for SERS-based analysis. A LOD of 0.1138 μg·mL^{-1} for tartrazine detection and the linear response range from 0.3 to 10 μg·mL^{-1} were obtained. The fingerprint recognition capability of SERS is conceivable to achieve high molecular selectivity and specificity with the functionalization of affinity ligands.

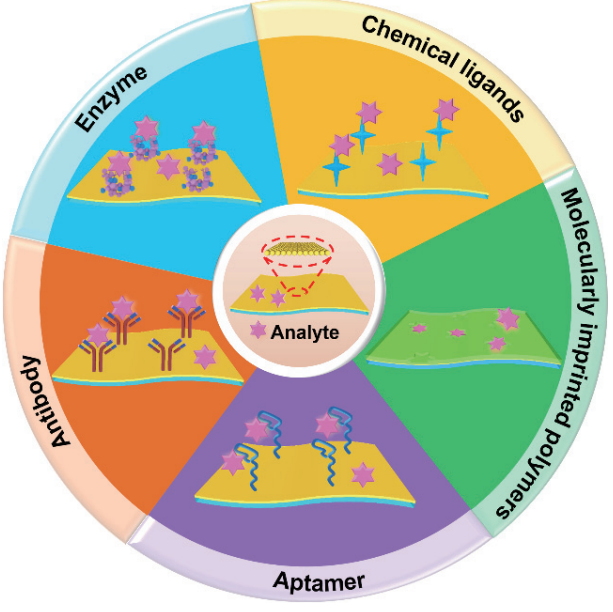

Figure 5 Ligands employed to anchor analyte for improving specificity.

4.3 Reusability

Reusability is an attractive and critical property in practical SERS detection [189], which makes the flexible SERS sensors reproducible and affordable [190]. To accomplish reusability, three challenges need to be solved. (1) Analytes from the last experiment should be removed or degraded as clear as possible, making sure they would not affect the next test. (2) The mechanical strength of surficial nanostructure should be ensured to endure repetitive experiments. (3) Many flexible, reusable SERS substrates are designed for point-of-care testing, thus the way to refresh substrate is supposed to be simple, user friendly, and affordable.

Up to now, many methods have been applied to regenerate SERS substrate, such as heat treatment, oxidative plasma cleaning, washing with agent, photocatalytic regeneration [191]. Most of the simple post-treatments always need carefully handling by specialists to effectively remove the adsorbed analytes from the substrate. Photocatalytic semiconductors, such as ZnO [192], Fe_2O_3 [82], and TiO_2 [83] are utilized to provide the substrate with reusability. However, their chemical enhancement (CM) for SERS signal is not strong enough and always needs to be integrated with electromagnetic enhancement (EM) provided by noble metal NPs. The electrons of semiconductors can be excited by incident light

from valence band to conduction band, and while holes are generated in valence band [193], which contribute to the generation of free radicals, such as superoxide radical anions ($O_2^{\cdot-}$) and hydroxyl radicals (·OH) [190, 194, 195]. These free radicals can induce adsorbed molecules degradation by redox reactions [196]. Small molecular degradation productions would be washed away, thus resulting in a clean substrate for the next test. Zhu et al. developed a flexible and reusable TiO_2 nanotube array film coated with AgNPs for formaldehyde (FA) measurement [197]. After SERS-based measurements, FA and 4-amino-3-hydrazino-5-mercapto-1,2,4-triazole (AHMT) were oxidized by free radicals which are generated under ultraviolet (UV) light. The adsorbed molecules were degraded down to an undetectable level after 190 min of UV radiation, presenting the feasibility of the substrate as a reusable pad. In addition to the degradation of the attached analytes, superhydrophobic surface with self-cleaning ability has also been reported [85]. The superhydrophobic surface decreases the contact area, prevents sample droplet adhesion, and minimizes residual amount. This strategy doesn't need sample droplet evaporation, thereby simplifying sample pretreatment as well [160]. Nevertheless, it means that the laser should be focused on an unpinned droplet instead of a stable surface area, which may limit its feasibility in real use.

A highly strong adherence between the supporting material and the active nanostructures is required, in case of the destruction of plasmonic nanostructure while washing out residuals. Embedding plasmonic NPs in the flexible substrate physically will significantly enhance the stability of the SERS sensor [141, 198]. Park et al. obtained a mechanically durable flexible substrate by decorating PDMS with Au nanostars [98]. Because the Au nanostar layer was fully embedded within the PDMS film, it displayed stable SERS enhancement after 100 cycles of stretching, bending, and torsion. The adherence strength between the supporting material and active nanostructures can also be enhanced by modification. Yang et al. demonstrated a cotton fabric-based substrate with firm reduced graphene oxide (rGO) coating [199]. They applied a coupling agent with three silanol groups (–Si–OH) to modify the supporting cotton. Silanol groups of the coupling agent dehydrated with the hydroxyl groups on the cotton surface, and the carboxyl and the hydroxyl groups of rGO, thereby greatly enhancing the action force between the cotton and the rGO. This strong interaction enables the substrate to keep its activity even after 40 times of rinsing and ultrasonic washing cycles.

5 Applications

SERS has gained great attention due to the ultrahigh sensitivity, rapid response time, and non-destructive molecular analysis. These features make SERS applicable to rapid, label-free identification of analytes. SERS-based flexible sensors with curve surface adaptability and low cost show significant promising applications in various fields, such as medical diagnostics, environmental analyses, food safety, forensic science, and so on.

5.1 Medical diagnostics

Flexible SERS-based sensors have been used to detect disease-related biomarkers for the diagnosis and screening of various diseases, such as cancer [200], jaundice [200], and gouty arthritis [201]. Trace-level detection of biomarkers benefits the diagnosis of diseases at an early stage. SERS-based platforms have achieved promising research results in the diagnosis of a variety of cancers by identifying the presence of cancer-related biomarkers in biofluids. Pimporn et al. used a paper-based SERS platform, combined with magnetic separation technology, to identify and verify colon cancer cells, achieving accuracy as high as 98% [174]. The technology provides a convenient, fast, and economical method for the diagnosis of cancer. Carcinoembryonic antigen (CEA) as a tumor marker in the blood or other bodily fluids is primarily associated with certain cancers. SERS-based lateral flow immunoassay (LFIA) strip composed of hydrophilic–hydrophobic Ag-modified PMMA substrate was developed for quantitative detection of CEA [202]. The results demonstrated that the flexible SERS strip had great potential for point-of-care (POC) diagnosis. Paper-based SERS substrate has been developed for the low-level detection of biomarkers in tuberculosis diagnostics [203], which meets the global challenges in fighting infectious diseases. Jaundice is one of the leading causes of death for newborn babies. A high level of bilirubin in blood (> 50 μM) potentially causes lethal consequences. Taking advantage of the strong adsorbability and fluorescence super quenching capability of graphene oxide-plasmonic gold nanostar (GO-GNS) hybrids, Xiang et al. developed a SERS biosensor based on GO-GNS modified paper for label-free detection of free bilirubin in blood serum for the jaundice diagnosis [117]. The biosensor was capable of achieving two different linear responses in the range of 5.0–150 and 150–500 μM, and a detection limit as low as 0.436 μM. Likewise, SERS sensors have also been employed in early prediction for prenatal diseases by finding biomarkers in amniotic fluids [204]. As shown in Fig. 6(a), a flexible SERS sensor was constructed by decorating AuNPs on ZnO nanorod arrays vertically grown on cellulose paper for analysis of amniotic fluids to detect prenatal diseases. The low-cost and disposable POC device enhanced the Raman signal by 1.25×10^7 with excellent reproducibility, and identified the types of diseases from amniotic fluids with > 92% clinical sensitivity and specificity, showing potential for identifying and predicting any amniotic-fluid-mediated diseases. Human tears contain assorted biochemical molecules. The level of uric acid in tears has a strong correlation with the level of uric acid in the blood, which is an indicator for non-invasive diagnosis of gouty arthritis. Park et al. developed a plasmonic Schirmer strip composed of cellulose fibers with evenly distributed gold nano islands to detect uric acid in human tears for gouty arthritis diagnosis using SERS (Fig. 6(b)) [21]. The SERS-based plasmonic diagnostic strip allowed an efficient collection of human tears because of the fast-wicking property of cellulose fiber matrices, and achieved quantitative detection of uric acid in human tears at physiological levels (25–150 μM). Vinayak et al. created a flexible plasmonic substrate with spatially controlled electromagnetic hot spots for screening of uric acid in human tears [205]. In conjunction with wearable electronics, flexible SERS sensors can construct a new generation of multifunctional devices. Wang et al. provided a wearable electronic sweat analysis device [206]. As shown in Fig. 6(c), the whole system consisted of a flexible SERS-active sensor for screening extracted targets in sweat and a flexible electronic device capable of automatic sweat extraction, which is capable of noninvasive molecule monitoring. The integrated wearable system exhibited a universal, sensitive tracking of important biomarkers or drug concentration inside the body, building a bridge to personalized diagnosis or therapy. Flexible SERS provides a cost-effective, scalable, and label-free method toward noninvasively detecting biomolecules from human fluids for POC diagnosis.

5.2 Environmental analyses

Pollution of water, air, soil caused by toxic chemicals results in a series of human health problems, which has aroused more and more concerns. Flexible SERS technique propels the development of fast and precise detection and identification of trace pollutants, such as heavy metals ions [207], organic pollutants [197, 208], and antibiotics [209, 210]. Lu et al. fabricated carbon fiber cloth

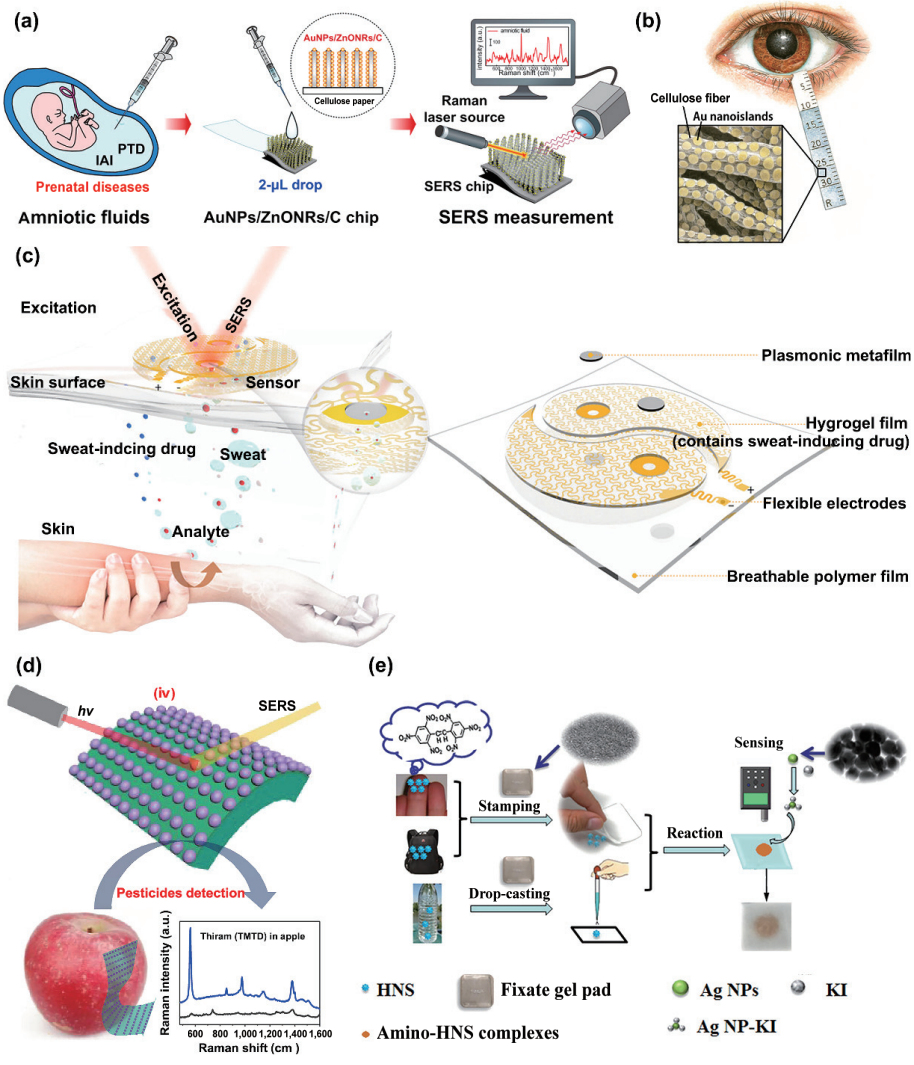

Figure 6 Applications of the flexible SERS platforms. (a) Flexible SERS chip composed of AuNPs/ZnONRs/C for amniotic fluids screening. Reproduced with permission from Ref. [204], © American Chemical Society 2018. (b) Schematic illustration of plasmonic Schirmer strip for SERS-based tear analysis. Reproduced with permission from Ref. [21], © American Chemical Society 2016. (c) Diagram of the working principle and design of the wearable plasmonic-electronic integrated sensing platform composed of sweat extraction component and SERS sensing component. Reproduced with permission from Ref. [206], © Wang, Y. L. et al. 2021. (d) Schematic drawing showing direct sampling and SERS-based analysis of pesticide on an apple. Reproduced with permission from Ref. [129], © American Chemical Society 2020. (e) Schematic diagram shows the SERS detection of HNS based on a fixate gel pad using a portable Raman spectrometer. Reproduced with permission from Ref. [173] © American Chemical Society 2020.

modified with silver nanodendrites as SERS substrate for detecting multiple kinds of pesticides in lake water rapidly and simultaneously [160]. The micro/nanostructures provided by fibers and nanodendrites made the flexible substrate super-hydrophobic, which facilitated the detection of analyte solution in form of a droplet on the superhydrophobic surface without pretreatment, and greatly shortened the detection time. Thiram and malachite green were distinguished simultaneously in real lake water. The water pollution caused by the misuse of antibiotics has posed a threat to the health of aquatic animals and human beings, which has become a serious problem that needs to be addressed urgently. SERS sensor for *in-situ* detection of furazolidone (FZD), an antibacterial drug that can cause water pollution, was proposed by Sun et al. [210]. The hydrophilic and hydrophobic pattern of the sensor helped to get rid of the limitation of diffusion and to enrich analytes. This method could be used for *in-situ* detection of FZD in different water areas or on surfaces of aquatic animals. Formaldehyde, identified as a carcinogen, is the most common and the best-known indoor air pollutant [211]. Sensitive and rapid analysis of formaldehyde is of great need for assessing environmental and human health risks. Zhu et al. provided a new type of silver-plated titanium dioxide nanotube array as flexible SERS substrate for highly sensitive detection of formaldehyde [197], achieving a LOD of 1.21×10^{-7} M. The excellent photocatalytic degradation performance and SERS activity of the substrate show great potential for the on-site detection and degradation of organic pollutants. Sun et al. recently reported a Au NPs immobilized PVDF SERS substrate for both water and air pollutants monitoring using a portable Raman spectrometer [212]. The inherent breathability of PVDF and flexible sheet structure enable gaseous and aqueous samples to pass through the substrate, thereby realizing continuous dynamic SERS measurement. The change of pH in a liquid environment or cigarette smoke in the air can be detected within 30 s. Flexible SERS technique with cost-effectiveness, high sensitivity, and high stability, provides large area *in-situ* sampling and screening for POC detection of detrimental substances in water, air, and soil.

5.3 Food safety

Modern food is characterized by complex ingredients and diverse textures, and its processing is often faced with the risk of natural and man-made pollution. SERS is a particularly effective food analysis technology due to its active and adjustable swab sampling

strategy and *in-situ* detection [26]. Pesticide contamination on food potentially results in serious health problems. The quantitative analysis of trace pesticides in agricultural products is important for the assessment of related food safety and human health. Guo et al. developed a gold NPs immobilized commercial adhesive tape for rapid extraction and detection of pesticide residues on fruits and vegetables [54]. The SERS tape offers the feasibility of simple sampling on complex surface, and *in situ* record of molecular structure information for the rapid detection of pesticides. However, flexible SERS sensors usually confront the problem of the quick degradation of their sensitivity and stability because of the low adhesion between plasmonic nanostructures and flexible substrates during swab sampling. Liu et al. developed a PI-based SERS sensor with high signal homogeneity and stability for detecting thiram pesticide (Fig. 6(d)) [129]. The SERS sensor composed of densely and uniformly distributed Ag@Au NPs embedded on a PI film showed excellent efficiency for trace pesticide detection on apple surfaces, and exhibited great durability after 30 days of storage. Animal feed contains crystalline violet, a kind of dose-related carcinogen, which has a high risk to cause liver cancer, certain adenomas, and sarcomas in humans. A flexible and transparent SERS substrate for the detection of crystalline violet on fish skin was provided by Li et al. Plasmonic Ag nanocube arrays were anchored onto a flexible and transparent PDMS membrane by self-assembly [213]. The flexible substrate has excellent transparency and flexibility, allowing conformal contact with non-planar surfaces, and permitting laser penetration from the backside of the substrate to the analyte. The properties facilitate *in situ* detection of trace residual crystalline violet on fish skin. Choline, a type of vitamin B, is an essential nutrient for the human body. The lack of choline in the body may lead to fatty liver, atherosclerosis, and Alzheimer's disease [214]. It is necessary to add choline to the diet of infants to improve their memory. Therefore, the quantitative measurement of choline in infant foods has received intensive attention. Weng et al. provided a flexible SERS method using a syringe filter and Ag triangular nanoplates for the detection of choline in infant milk [215]. The flexible SERS substrate, combined with SERS marker transformation, showed high SERS activity and excellent reproducibility, achieving detectable concentrations ranging from 10^{-3} to 10^{-7} M and an effective detection limit as low as 8.36 nM. Flexible SERS sensors as portable and low-cost devices are preferable candidates in realizing ultrasensitive detection of food contamination in practical applications.

5.4 Forensic science

With the urgent need of security check and criminal forensic authentication, timely and reliable explosive detection strategy has become more and more attractive in recent years. SERS technology, owing to its high resolution, photobleaching resistance, real-time, and non-invasive, has been proved to be a powerful analytical tool for trace detection of diverse hazardous or toxic chemicals. TNT has been known as the "king of explosives" because of its highly powerful energy, and is considered to be environmental "ticking bombs". Trace detection of TNT provides a crucial indication for decontamination action and early warning of criminal forensic. Li et al. detected TNT on a flexible Ag-nanoparticle decorated polyacrylonitrile nano-hump array film [216], obtaining a low LOD of 10^{-12} M. In order to achieve detection of extremely low traces of explosives, Wu et al. developed a 3D nanocellulose aerogels-based SERS sensor for sensing TNT [217], achieving EF as high as 1.87×10^8 and LOD down to 8×10^{-12} g·L^{-1}. The 3D porous substrate with a large surface area embedded with core–shell Au@Ag nanocubes leads to dense and uniform distribution of 3D hot spots, which greatly increases the sensitivity of the SERS sensor. Thakshila et al. fabricated a sensitive and stable SERS nanosensor for detection of three commonly military explosives (TNT, oxygen, and pentaerythritol tetranitrate) by self-assembling gold triangular nano-prisms onto a commercially available, flexible, and adhesive film [22]. Inorganic explosives, such as perchlorates (ClO_4^-), chlorates (ClO_3^-), or nitrates (NO_3^-) are well known for their high stability and non-volatility. A flexible sensor composed of positively charged silver nanowire membrane was provided by Shi et al. for trace detection of inorganic explosives using SERS in a swab-sampling manner [218]. It provides sensitive and on-site detection of inorganic explosives platform by using a portable Raman spectrometer. HNS is a more harmful explosive than TNT. The detection of HNS residue on surfaces is essential for security screening. Fan et al. developed a multifunctional flexible SERS sensor for on-site detection of HNS (Fig. 6(e)) [173]. The sticky nature of the flexible sensor enables it to efficiently collect HNS residues on surfaces. The SERS sensors achieved extraordinarily sensitive detection of HNS based on the profound enhancement with the potassium iodide-modified Ag NPs. Notably, the flexible SERS nanosensor enables direct sampling of explosive trace residues from real-world surfaces, which obviates the need of complicated sample processing. Flexible SERS-based methods show promising potential for applications in rapid safety inspection and military threats, thus will help to reduce the threat to public safety.

6 Advanced algorithms for SERS data processing

The identification and content analyses of substances are usually tedious and require experienced personnel, which limits the popularization and application of SERS. To deal with the large-scale datasets obtained from vibrational spectra of complex mixtures, especially data of biological samples with low signal-to-noise ratio (SNR), advanced data processing techniques are required to effectively extract meaningful information. Machine learning algorithms including unsupervised learning and supervised learning have been employed to recognize hard-to-distinguish features of SERS for interpretation and classification [219]. Consequently, plenty of advanced algorithms have been utilized in SERS analyses to intelligently distinguish the species and contents of analytes with high accuracy, sensitivity, and selectivity [220, 221].

6.1 Data preprocessing

SERS containing intrinsic Raman signals of multiple components may be obscured by interferences from fluorescence background, instruments, and other noise [222]. To achieve reliable spectra for further analysis, preprocessing is inevitable to subtract background disturbance and remove the artifact. Accordingly, noise suppression, baseline correction, and normalization are usually involved in the preprocessing step for raw spectral data. To improve the SNR, denoising approaches, such as Savitzky–Golay smoothing filter [223] and wavelet transform [224], can effectively reduce the impact of noises and retain the Raman signals [225]. Asymmetric least squares smoothing (AsLS) method with two turning parameters (λ and p) is a commonly used method to eliminate the potential baseline variability [226]. An improved method called adaptive iteratively reweighted penalized least squares (airPLS) is widely used in baseline correction for Raman spectra with no need of any prior information and individual intervention [227]. The airPLS method estimates baseline by an iteration strategy of adjusting the weight vector. There is only one intuitional and adjustable parameter λ in comparison to the AsLS.

The intensity of Raman spectrum is also affected by the fluctuation of laser intensity, the change of relative position between the probe and measured object, and the change of charge-coupled device (CCD) integration time. MinMax normalization, compressing the spectra into [0, 1] range, is necessary to remove laser power fluctuation and guarantees comparable intensities for each spectrum. The proper selection and combination of preprocessing algorithms benefit the performance of subsequent machine learning models.

6.2 Machine learning algorithms for analyses of SERS

Various forms of machine learning algorithms are considered to be powerful tools for capturing complex relationships within multivariate SERS spectra [228]. Unsupervised learning algorithms with no need of prior knowledge of spectral characteristics, such as principal component analysis (PCA) [229], clustering-based algorithms [230], are adopted to discover unknown features in SERS spectra without labeled datasets. Shin et al. identified the unique spectral peaks of non-small cell lung cancer cell-derived exosomes by utilizing PCA for cancer diagnosis, and verified the Raman patterns through ratiometric analysis of mixtures of cancerous and normal exosomes [229]. Lim et al. applied PCA to identify cells infected with different influenza viruses based on label-free SERS, which provides a precise and sensitive diagnostic method for early identification of newly emerging viruses [231].

Supervised learning algorithms, such as random forest (RF), support vector machine (SVM), and K-nearest neighbors (KNN), logistic regression, discriminant analysis, and neural networks, have been utilized to intelligently distinguish the species and content of analytes with high accuracy, sensitivity, and selectivity. These methods can be trained to recognize features in Raman (or SERS) spectra, and facilitate species and strains discrimination with a prior knowledge of classification groups [219]. To improve the accuracy and efficiency of learning algorithms, dimensionality reduction methods are applied to reduce the large redundant data [232]. Feng et al. employed PCA to reduce data collinearity and identify the principal components, and then applied linear discriminant analysis (LDA) to discriminate cancerous samples from normal samples [233]. The empirical diagnostic algorithm based on PCA-LDA achieved diagnostic sensitivity of 96.7% and a specificity of 92%. SVM, an effectively used discrimination model, generates optimal hyperplane in high dimensional spaces to realize linear separability using kernel functions [234, 235]. Li et al. applied three SVM models with three kernel functions including linear, polynomial, and Gaussian radial basis function (RBF) to distinguish SERS spectra of serum from prostate cancer patients and healthy persons [236]. Compared to the PCA-LDA classifiers with accuracy of 91.3% and area under the curve (AUC) value of 0.991, the RBF kernel SVM model shows relatively higher performance with accuracy of 98.8% and AUC value of 0.998. Notably, choosing proper kernel for the specific task is a necessary process. Although SVM is capable of handling non-linear and multi-category classification, it is less realistic to train an SVM model adaptive to large-scale spectral analyses involving plenty of classes. Machine learning methods become unwieldy on high-resolution and high-dimensional SERS datasets.

6.3 Deep learning models for analyses of SERS

Deep learning also known as deep neural networks, is a subset of machine learning [238], showing superior performance to analyze spectroscopic signals [239]. Deep learning models provide avenues to extract features and discover subtle differences from the intricate structure of high-dimensional raw spectra datasets [240]. Deep neural networks composed of many nonlinear modules can learn critical patterns hierarchically and transform these patterns to more abstract and higher-level representations, which confers high analytical performance [241]. Convolutional neural network (CNN), as a predominant deep learning tool for SERS interpretation, revolutionizes the information-rich SERS analyses for complex scenarios [242], and reduces the need for data preprocessing and highlighting important variations inside the spectra, both of which are key steps in the analyses of SERS data [243]. To guarantee the veracity and adaptability of input spectral data conducted by deep learning neural networks, it is advisable to minimize the background signal of autofluorescence and normalize the spectra within the interest spectral range [241]. Erzina et al. combined the specific SERS and CNN to detect biochemical changes in culture medium arising from metabolic activity, thus identifying melanoma and normal cells [244]. Three categories of SERS spectra of cells cultivation media were generated as enhanced input to train CNN model. The CNN model achieved 100% accuracy in the discrimination of tumor and normal cell cultivation media. For analysis of complex and heterogeneous composition of human blood exosomes, Shin et al. employed deep learning-based SERS analysis to recognize healthy or diseased cells for early-stage liquid biopsy of lung cancer [237]. As shown in Fig. 7, the spectral data of supernatant exosomes from normal cells and cancer cells were used as input to train the deep learning model for binary classification with accuracy of 94.8% on average. They further combined the model with PCA to predict human plasma-derived exosomes for early-stage diagnosis of lung cancer with accuracy of 90.7%. Deep learning neural networks possessing well-designed architecture embedded with regularization techniques can reduce the overfitting risk and improve the robustness effectively. With advances in improving interpretability and repeatability for limited spectra samples, deep learning algorithms will have a more significant impact on SERS analysis in a high sensitivity and specificity manner, especially in label-free, onsite, and real-time clinical decisions according to the up-to-date trends.

7 Conclusion and prospects

The increasingly demanded POC diagnostics has stimulated unprecedented advances of flexible SERS technique, which is capable of attachment on arbitrary surfaces, allowing onsite and real-time monitoring. This progress report provides a systematic survey on the state-of-art in flexible SERS sensors. Various kinds of flexible substrates used in SERS sensors are systematically summarized. Rational design and fabrication of structurally uniform SERS sensitive nanostructures on the flexible substrates are discussed in depth. Strategies for constructing flexible SERS sensors toward POC detection are also discussed broodingly and thoroughly. The applications of the flexible SERS technique emerging in biological diagnosis, environmental analysis, food safety, and forensic science are elaborated. In addition, advanced data processing techniques as auxiliary means are deeply analyzed. SERS data analysis usually suffers from complexity in spectral interpretation. The advanced data processing models are adopted to recognize hard-to-distinguish features of SERS data for interpretation and classification, especially data of biological samples with low signal-to-noise ratio.

Despite SERS-based sensing platform having achieved blooming advances, there is still a plurality of challenges to be overcome for effective and accurate POC diagnostics. Firstly, to fulfill a real-life task, the stability of the substrates and the nano-architectures should be evaluated with at least months rather than days by considering multiple factors such as oxidation, temperature, pH, and ionic strength. Secondly, standardized procedures and methodologies for low-cost fabrication of SERS

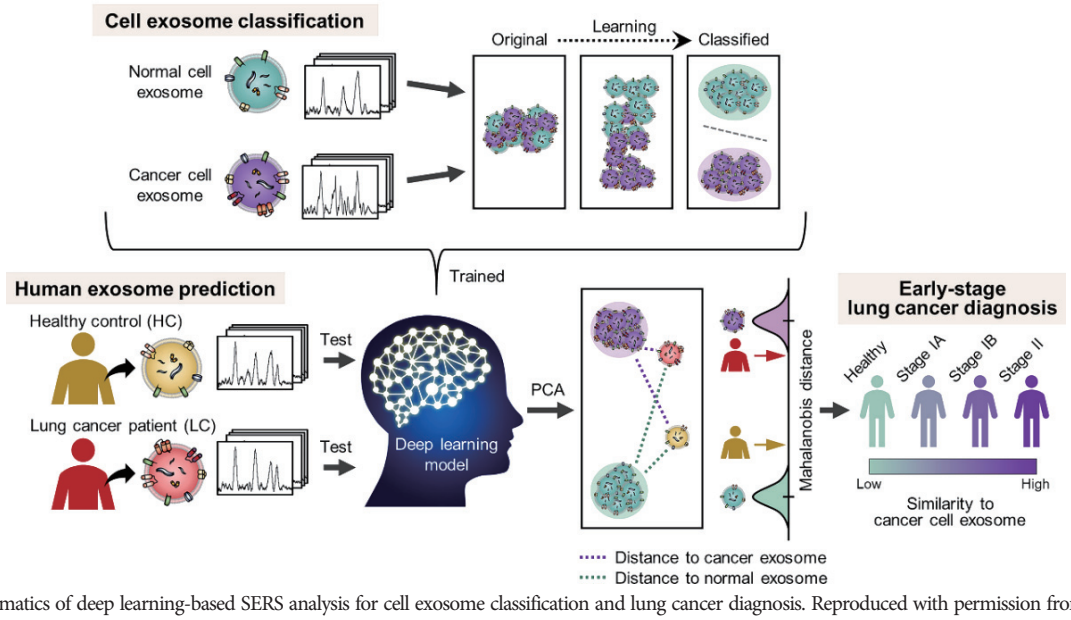

Figure 7 Schematics of deep learning-based SERS analysis for cell exosome classification and lung cancer diagnosis. Reproduced with permission from Ref. [237], © American Chemical Society 2020.

devices with batch-to-batch consistency and large-scale production are highly desirable. Thirdly, although deep learning models display good performance for processing the intricate structure of high-dimensional raw spectra datasets, the veracity of spectral datasets is indispensably needed to guarantee the accuracy of results. Meanwhile, the repeatability of analysis results and the robustness of models can be facilitated using sufficient datasets with high-quality data. In particular, integrated with a handheld portable Raman spectrometer [245], reproducible SERS sensors in combination with microfluidic technology, wearable techniques, or nanotechnology, promisingly facilitate the flexible SERS technology from a laboratory-based tool to a practical real-world analysis platform, and open up new horizons in various fields.

Acknowledgments

This work was financially supported by the Fundamental Research Funds for the Central Universities (No. N2019008) and the National Natural Science Foundation of China (No. 81501556).

References

[1] Fleischmann, M.; Hendra, P. J.; McQuillan, A. J. Raman spectra of pyridine adsorbed at a silver electrode. *Chem. Phys. Lett.* **1974**, *26*, 163–166.

[2] Ding, S. Y.; Yi, J.; Li, J. F.; Ren, B.; Wu, D. Y.; Panneerselvam, R.; Tian, Z. Q. Nanostructure-based plasmon-enhanced Raman spectroscopy for surface analysis of materials. *Nat. Rev. Mater.* **2016**, *1*, 16021.

[3] Kneipp, K.; Wang, Y.; Kneipp, H.; Itzkan, I.; Dasari, R. R.; Feld, M. S. Population pumping of excited vibrational states by spontaneous surface-enhanced Raman scattering. *Phys. Rev. Lett.* **1996**, *76*, 2444–2447.

[4] Zong, C.; Xu, M. X.; Xu, L. J.; Wei, T.; Ma, X.; Zheng, X. S.; Hu, R.; Ren, B. Surface-enhanced Raman spectroscopy for bioanalysis: Reliability and challenges. *Chem. Rev.* **2018**, *118*, 4946–4980.

[5] Garcia-Rico, E.; Alvarez-Puebla, R. A.; Guerrini, L. Direct surface-enhanced Raman scattering (SERS) spectroscopy of nucleic acids: From fundamental studies to real-life applications. *Chem. Soc. Rev.* **2018**, *47*, 4909–4923.

[6] Camden, J. P.; Dieringer, J. A.; Wang, Y. M.; Masiello, D. J.; Marks, L. D.; Schatz, G. C.; Van Duyne, R. P. Probing the structure of single-molecule surface-enhanced Raman scattering hot spots. *J. Am. Chem. Soc.* **2008**, *130*, 12616–12617.

[7] Laing, S.; Jamieson, L. E.; Faulds, K.; Graham, D. Surface-enhanced Raman spectroscopy for *in vivo* biosensing. *Nat. Rev. Chem.* **2017**, *1*, 0060.

[8] Zeng, Y.; Koo, K. M.; Trau, M.; Shen, A. G.; Hu, J. M. Watching SERS glow for multiplex biomolecular analysis in the clinic: A review. *Appl. Mater. Today* **2019**, *15*, 431–444.

[9] Lenzi, E.; De Aberasturi, D. J.; Liz-Marzán, L. M. Surface-enhanced Raman scattering tags for three-dimensional bioimaging and biomarker detection. *ACS Sens.* **2019**, *4*, 1126–1137.

[10] Luo, S. C.; Sivashanmugan, K.; Liao, J. D.; Yao, C. K.; Peng, H. C. Nanofabricated SERS-active substrates for single-molecule to virus detection *in vitro*: A review. *Biosens. Bioelectron.* **2014**, *61*, 232–240.

[11] Cialla-May, D.; Zheng, X. S.; Weber, K.; Popp, J. Recent progress in surface-enhanced Raman spectroscopy for biological and biomedical applications: From cells to clinics. *Chem. Soc. Rev.* **2017**, *46*, 3945–3961.

[12] Bruzas, I.; Lum, W.; Gorunmez, Z.; Sagle, L. Advances in surface-enhanced Raman spectroscopy (SERS) substrates for lipid and protein characterization: Sensing and beyond. *Analyst* **2018**, *143*, 3990–4008.

[13] Nie, S. M.; Emory, S. R. Probing single molecules and single nanoparticles by surface-enhanced Raman scattering. *Science* **1997**, *275*, 1102–1106.

[14] Albrecht, M. G.; Creighton, J. A. Anomalously intense Raman spectra of pyridine at a silver electrode. *J. Am. Chem. Soc.* **1977**, *99*, 5215–5217.

[15] Xu, K. C.; Zhou, R.; Takei, K.; Hong, M. H. Toward flexible surface-enhanced Raman scattering (SERS) sensors for point-of-care diagnostics. *Adv. Sci.* **2019**, *6*, 1900925.

[16] Restaino, S. M.; White, I. M. A critical review of flexible and porous SERS sensors for analytical chemistry at the point-of-sample. *Anal. Chim. Acta* **2019**, *1060*, 17–29.

[17] Ma, Y.; Chen, Y.; Tian, Y. R.; Gu, C. J.; Jiang, T. Contrastive study of *in situ* sensing and swabbing detection based on SERS-active gold nanobush-PDMS hybrid film. *J. Agric. Food Chem.* **2021**, *69*, 1975–1983.

[18] Kang, H.; Heo, C. J.; Jeon, H. C.; Lee, S. Y.; Yang, S. M. Durable plasmonic cap arrays on flexible substrate with real-time optical tunability for high-fidelity SERS devices. *ACS Appl. Mater. Interfaces* **2013**, *5*, 4569–4574.

[19] Xu, K. C.; Wang, Z. Y.; Tan, C. F.; Kang, N.; Chen, L. W.; Ren, L.; Thian, E. S.; Ho, G. W.; Ji, R.; Hong, M. H. Uniaxially stretched flexible surface plasmon resonance film for versatile surface enhanced Raman scattering diagnostics. *ACS Appl. Mater. Interfaces* **2017**, *9*, 26341–26349.

[20] Wang, P.; Wu, L.; Lu, Z. C.; Li, Q.; Yin, W. M.; Ding, F.; Han, H.

Y. Gecko-inspired nanotentacle surface-enhanced Raman spectroscopy substrate for sampling and reliable detection of pesticide residues in fruits and vegetables. *Anal. Chem.* **2017**, *89*, 2424–2431.

[21] Park, M.; Jung, H.; Jeong, Y.; Jeong, K. H. Plasmonic schirmer strip for human tear-based gouty arthritis diagnosis using surface-enhanced Raman scattering. *ACS Nano* **2017**, *11*, 438–443.

[22] Liyanage, T.; Rael, A.; Shaffer, S.; Zaidi, S.; Goodpaster, J. V.; Sardar, R. Fabrication of a self-assembled and flexible SERS nanosensor for explosive detection at parts-per-quadrillion levels from fingerprints. *Analyst* **2018**, *143*, 2012–2022.

[23] Kalachyova, Y.; Erzina, M.; Postnikov, P.; Svorcik, V.; Lyutakov, O. Flexible SERS substrate for portable Raman analysis of biosamples. *Appl. Surf. Sci.* **2018**, *458*, 95–99.

[24] Shi, R. Y.; Liu, X. J.; Ying, Y. B. Facing challenges in real-life application of surface-enhanced Raman scattering: Design and nanofabrication of surface-enhanced Raman scattering substrates for rapid field test of food contaminants. *J. Agric. Food Chem.* **2018**, *66*, 6525–6543.

[25] Polavarapu, L.; Liz-Marzán, L. M. Towards low-cost flexible substrates for nanoplasmonic sensing. *Phys. Chem. Chem. Phys.* **2013**, *15*, 5288–5300.

[26] Zhang, D. R.; Pu, H. B.; Huang, L. J.; Sun, D. W. Advances in flexible surface-enhanced Raman scattering (SERS) substrates for nondestructive food detection: Fundamentals and recent applications. *Trends Food Sci. Technol.* **2021**, *109*, 690–701.

[27] Liu, H. Q.; He, Y. N.; Cao, K. Z. Flexible surface-enhanced Raman scattering substrates: A review on constructions, applications, and challenges. *Adv. Mater. Interfaces* **2021**, *8*, 2100982.

[28] Li, Z. Y.; Huang, X.; Lu, G. Recent developments of flexible and transparent SERS substrates. *J. Mater. Chem. C* **2020**, *8*, 3956–3969.

[29] Wei, H. R.; Abtahi, S. M. H.; Vikesland, P. J. Plasmonic colorimetric and SERS sensors for environmental analysis. *Environ. Sci. :Nano* **2015**, *2*, 120–135.

[30] Campion, A.; Kambhampati, P. Surface-enhanced Raman scattering. *Chem. Soc. Rev.* **1998**, *27*, 241–250.

[31] Cardinal, M. F.; Ende, E. V.; Hackler, R. A.; McAnally, M. O.; Stair, P. C.; Schatz, G. C.; Van Duyne, R. P. Expanding applications of SERS through versatile nanomaterials engineering. *Chem. Soc. Rev.* **2017**, *46*, 3886–3903.

[32] Han, X. X.; Ji, W.; Zhao, B.; Ozaki, Y. Semiconductor-enhanced Raman scattering: Active nanomaterials and applications. *Nanoscale* **2017**, *9*, 4847–4861.

[33] Jensen, L.; Aikens, C. M.; Schatz, G. C. Electronic structure methods for studying surface-enhanced Raman scattering. *Chem. Soc. Rev.* **2008**, *37*, 1061–1073.

[34] Phan-Quang, G. C.; Han, X. M.; Koh, C. S. L.; Sim, H. Y. F.; Lay, C. L.; Leong, S. X.; Lee, Y. H.; Pazos-Perez, N.; Alvarez-Puebla, R. A.; Ling, X. Y. Three-dimensional surface-enhanced Raman scattering platforms: Large-scale plasmonic hotspots for new applications in sensing, microreaction, and data storage. *Acc. Chem. Res.* **2019**, *52*, 1844–1854.

[35] Huang, Y.; Zhang, X.; Ringe, E.; Ma, L. W.; Zhai, X.; Wang, L. L.; Zhang, Z. J. Detailed correlations between SERS enhancement and plasmon resonances in subwavelength closely spaced Au nanorod arrays. *Nanoscale* **2018**, *10*, 4267–4275.

[36] McFarland, A. D.; Young, M. A.; Dieringer, J. A.; Van Duyne, R. P. Wavelength-scanned surface-enhanced Raman excitation spectroscopy. *J. Phys. Chem. B* **2005**, *109*, 11279–11285.

[37] Yang, L. L.; Peng, Y. S.; Yang, Y.; Liu, J. J.; Huang, H. L.; Yu, B. H.; Zhao, J. M.; Lu, Y. L.; Huang, Z. R.; Li, Z. Y. et al. A novel ultra-sensitive semiconductor SERS substrate boosted by the coupled resonance effect. *Adv. Sci.* **2019**, *6*, 1900310.

[38] Wang, Y. C.; Jin, Y. H.; Xiao, X. Y.; Zhang, T. F.; Yang, H. T.; Zhao, Y. D.; Wang, J. P.; Jiang, K. L.; Fan, S. S.; Li, Q. Q. Flexible, transparent and highly sensitive SERS substrates with cross-nanoporous structures for fast on-site detection. *Nanoscale* **2018**, *10*, 15195–15204.

[39] Gao, R. K.; Song, X. F.; Zhan, C. B.; Weng, C. G.; Cheng, S.; Guo, K.; Ma, N.; Chang, H. F.; Guo, Z. Y.; Luo, L. B. et al. Light trapping induced flexible wrinkled nanocone SERS substrate for highly sensitive explosive detection. *Sens. Actuators B:Chem.* **2020**, *314*, 128081.

[40] Jiao, L. Y.; Fan, B.; Xian, X. J.; Wu, Z. Y.; Zhang, J.; Liu, Z. F. Creation of nanostructures with poly(methyl methacrylate)-mediated nanotransfer printing. *J. Am. Chem. Soc.* **2008**, *130*, 12612–12613.

[41] Hatab, N. A. A.; Oran, J. M.; Sepaniak, M. J. Surface-enhanced Raman spectroscopy substrates created via electron beam lithography and nanotransfer printing. *ACS Nano* **2008**, *2*, 377–385.

[42] Zhao, X. F.; Yu, J.; Zhang, C.; Chen, C. S.; Xu, S. C.; Li, C. H.; Li, Z.; Zhang, S. Z.; Liu, A. H.; Man, B. Y. Flexible and stretchable SERS substrate based on a pyramidal PMMA structure hybridized with graphene oxide assivated AgNPs. *Appl. Surf. Sci.* **2018**, *455*, 1171–1178.

[43] Wu, S. J.; Duan, N.; Shen, M. F.; Wang, J.; Wang, Z. P. Surface-enhanced Raman spectroscopic single step detection of *Vibrio parahaemolyticus* using gold coated polydimethylsiloxane as the active substrate and aptamer modified gold nanoparticles. *Microchim. Acta* **2019**, *186*, 401.

[44] Ma, Y.; Du, Y. Y.; Chen, Y.; Gu, C. J.; Jiang, T.; Wei, G. D.; Zhou, J. Intrinsic Raman signal of polymer matrix induced quantitative multiphase SERS analysis based on stretched PDMS film with anchored Ag nanoparticles/Au nanowires. *Chem. Eng. J.* **2020**, *381*, 122710.

[45] Cheng, Y. W.; Hsiao, C. W.; Zeng, Z. L.; Syu, W. L.; Liu, T. Y. The interparticle gap manipulation of Au-Ag nanoparticle arrays deposited on flexible and atmospheric plasma-treated PDMS substrate for SERS detection. *Surf. Coat. Technol.* **2020**, *389*, 125653.

[46] Zhang, H.; Zhang, W.; Xiao, L. F.; Liu, Y.; Gilbertson, T. A.; Zhou, A. H. Use of surface-enhanced Raman scattering (SERS) probes to detect fatty acid receptor activity in a microfluidic device. *Sensors* **2019**, *19*, 1663.

[47] Ariaeenejad, S.; Hosseini, E.; Motamedi, E.; Moosavi-Movahedi, A. A.; Salekdeh, G. H. Application of carboxymethyl cellulose-g-poly(acrylic acid-co-acrylamide) hydrogel sponges for improvement of efficiency, reusability and thermal stability of a recombinant xylanase. *Chem. Eng. J.* **2019**, *375*, 122022.

[48] Ahn, S.; Lee, S. J. Nano/micro natural patterns of hydrogels against water loss. *ACS Appl. Bio Mater.* **2020**, *3*, 1293–1304.

[49] He, Y.; Yang, X.; Yuan, R.; Chai, Y. Q. Switchable target-responsive 3D DNA hydrogels as a signal amplification strategy combining with SERS technique for ultrasensitive detection of miRNA 155. *Anal. Chem.* **2017**, *89*, 8538–8544.

[50] He, X.; Zhou, X.; Liu, W.; Liu, Y.; Wang, X. L. Flexible DNA hydrogel SERS active biofilms for conformal ultrasensitive detection of uranyl ions from aquatic products. *Langmuir* **2020**, *36*, 2930–2936.

[51] Wang, C.; Wong, K. W.; Wang, Q.; Zhou, Y. F.; Tang, C. Y.; Fan, M. K.; Mei, J.; Lau, W. M. Silver-nanoparticles-loaded chitosan foam as a flexible SERS substrate for active collecting analytes from both solid surface and solution. *Talanta* **2019**, *191*, 241–247.

[52] Fu, H. P.; Chen, J. M.; Chen, L. J.; Zhu, X.; Chen, Z. L.; Qiu, B.; Lin, Z. Y.; Guo, L. H.; Chen, G. N. A calcium alginate sponge with embedded gold nanoparticles as a flexible SERS substrate for direct analysis of pollutant dyes. *Microchim. Acta* **2019**, *186*, 64.

[53] Sun, J.; Gong, L.; Lu, Y. T.; Wang, D. M.; Gong, Z. J.; Fan, M. K. Dual functional PDMS sponge SERS substrate for the on-site detection of pesticides both on fruit surfaces and in juice. *Analyst* **2018**, *143*, 2689–2695.

[54] Chen, J. M.; Huang, Y. J.; Kannan, P.; Zhang, L.; Lin, Z. Y.; Zhang, J. W.; Chen, T.; Guo, L. H. Flexible and adhesive surface enhance Raman scattering active tape for rapid detection of pesticide residues in fruits and vegetables. *Anal. Chem.* **2016**, *88*, 2149–2155.

[55] Sitjar, J.; Liao, J. D.; Lee, H.; Pan, L. P.; Liu, B. H.; Fu, W. E.; Chen, G. D. Ag nanostructures with spikes on adhesive tape as a

flexible SERS-active substrate for *in situ* trace detection of pesticides on fruit skin. *Nanomaterials* **2019**, *9*, 1750.
[56] Liu, X. J.; Wang, J. J.; Wang, J. J.; Tang, L. H.; Ying, Y. B. Flexible and transparent surface-enhanced Raman scattering (SERS)-active metafilm for visualizing trace molecules via Raman spectral mapping. *Anal. Chem.* **2016**, *88*, 6166–6173.
[57] Jiang, J. L.; Zou, S. M.; Li, Y. R.; Zhao, F. T.; Chen, J.; Wang, S. F.; Wu, H. X.; Xu, J. S.; Chu, M. F.; Liao, J. S. et al. Flexible and adhesive tape decorated with silver nanorods for *in-situ* analysis of pesticides residues and colorants. *Microchim. Acta* **2019**, *186*, 603.
[58] Pang, S.; Yang, T. X.; He, L. L. Review of surface enhanced Raman spectroscopic (SERS) detection of synthetic chemical pesticides. *TrAC Trends Anal. Chem.* **2016**, *85*, 73–82.
[59] Cate, D. M.; Adkins, J. A.; Mettakoonpitak, J.; Henry, C. S. Recent developments in paper-based microfluidic devices. *Anal. Chem.* **2015**, *87*, 19–41.
[60] Hansora, D. P.; Shimpi, N. G.; Mishra, S. Performance of hybrid nanostructured conductive cotton materials as wearable devices: An overview of materials, fabrication, properties and applications. *RSC Adv.* **2015**, *5*, 107716–107770.
[61] Xie, L. P.; Zi, X. Y.; Zeng, H.; Sun, J. J.; Xu, L. S.; Chen, S. Low-cost fabrication of a paper-based microfluidic using a folded pattern paper. *Anal. Chim. Acta* **2019**, *1053*, 131–138.
[62] Xiong, Z. Y.; Chen, X. W.; Liou, P.; Lin, M. S. Development of nanofibrillated cellulose coated with gold nanoparticles for measurement of melamine by SERS. *Cellulose* **2017**, *24*, 2801–2811.
[63] Ogundare, S. A.; Van Zyl, W. E. A review of cellulose-based substrates for SERS: Fundamentals, design principles, applications. *Cellulose* **2019**, *26*, 6489–6528.
[64] Yan, D.; Qiu, L. L.; Xue, M.; Meng, Z. H.; Wang, Y. F. A flexible surface-enhanced Raman substrates based on cellulose photonic crystal/Ag-nanoparticles composite. *Mater. Des.* **2019**, *165*, 107601.
[65] Oliveira, M. J.; Quaresma, P.; De Almeida, M. P.; Araújo, A.; Pereira, E.; Fortunato, E.; Martins, R.; Franco, R.; Águas, H. Office paper decorated with silver nanostars—An alternative cost effective platform for trace analyte detection by SERS. *Sci. Rep.* **2017**, *7*, 2480.
[66] Huang, L. Q.; Wu, C. J.; Xie, L. J.; Yuan, X.; Wei, X. Y.; Huang, Q.; Chen, Y. Q.; Lu, Y. D. Silver-nanocellulose composite used as SERS substrate for detecting carbendazim. *Nanomaterials* **2019**, *9*, 355.
[67] Chen, L. Y.; Ying, B. B.; Song, P. F.; Liu, X. Y. A nanocellulose-paper-based SERS multiwell plate with high sensitivity and high signal homogeneity. *Adv. Mater. Interfaces* **2019**, *6*, 1901346.
[68] Ballerini, D. R.; Ngo, Y. H.; Garnier, G.; Ladewig, B. P.; Shen, W.; Jarujamrus, P. Gold nanoparticle-functionalized thread as a substrate for SERS study of analytes both bound and unbound to gold. *AIChE J.* **2014**, *60*, 1598–1605.
[69] Gu, H. X.; Li, D. W.; Xue, L.; Zhang, Y. F.; Long, Y. T. A portable microcolumn based on silver nanoparticle functionalized glass fibers and its SERS application. *Analyst* **2015**, *140*, 7934–7938.
[70] Emamian, S.; Eshkeiti, A.; Narakathu, B. B.; Avuthu, S. G. R.; Atashbar, M. Z. Gravure printed flexible surface enhanced Raman spectroscopy (SERS) substrate for detection of 2, 4-dinitrotoluene (DNT) vapor. *Sens. Actuators B:Chem.* **2015**, *217*, 129–135.
[71] Mitomo, H.; Horie, K.; Matsuo, Y.; Niikura, K.; Tani, T.; Naya, M.; Ijiro, K. Active gap SERS for the sensitive detection of biomacromolecules with plasmonic nanostructures on hydrogels. *Adv. Opt. Mater.* **2016**, *4*, 259–263.
[72] Korkmaz, A.; Kenton, M.; Aksin, G.; Kahraman, M.; Wachsmann-Hogiu, S. Inexpensive and flexible SERS substrates on adhesive tape based on biosilica plasmonic nanocomposites. *ACS Appl. Nano Mater.* **2018**, *1*, 5316–5326.
[73] Kumar, S.; Goel, P.; Singh, J. P. Flexible and robust SERS active substrates for conformal rapid detection of pesticide residues from fruits. *Sens. Actuators B:Chem.* **2017**, *241*, 577–583.
[74] Kolluru, C.; Gupta, R.; Jiang, Q. S.; Williams, M.; Derami, H. G.; Cao, S. S.; Noel, R. K.; Singamaneni, S.; Prausnitz, M. R. Plasmonic paper microneedle patch for on-patch detection of molecules in dermal interstitial fluid. *ACS Sens.* **2019**, *4*, 1569–1576.
[75] Lee, M.; Oh, K.; Choi, H. K.; Lee, S. G.; Youn, H. J.; Lee, H. L.; Jeong, D. H. Subnanomolar sensitivity of filter paper-based SERS sensor for pesticide detection by hydrophobicity change of paper surface. *ACS Sens.* **2018**, *3*, 151–159.
[76] Xiong, Z. Y.; Lin, M. S.; Lin, H. T.; Huang, M. Z. Facile synthesis of cellulose nanofiber nanocomposite as a SERS substrate for detection of thiram in juice. *Carbohydr. Polym.* **2018**, *189*, 79–86.
[77] Parnsubsakul, A.; Ngoensawat, U.; Wutikhun, T.; Sukmanee, T.; Sapcharoenkun, C.; Pienpinijtham, P.; Ekgasit, S. Silver nanoparticle/bacterial nanocellulose paper composites for paste-and-read SERS detection of pesticides on fruit surfaces. *Carbohydr. Polym.* **2020**, *235*, 115956.
[78] Chen, J.; Huang, M. Z.; Kong, L. L.; Lin, M. S. Jellylike flexible nanocellulose SERS substrate for rapid *in-situ* non-invasive pesticide detection in fruits/vegetables. *Carbohydr. Polym.* **2019**, *205*, 596–600.
[79] Chen, J.; Huang, M. Z.; Kong, L. L. Flexible Ag/nanocellulose fibers SERS substrate and its applications for *in-situ* hazardous residues detection on food. *Appl. Surf. Sci.* **2020**, *533*, 147454.
[80] Kurita, M.; Arakawa, R.; Kawasaki, H. Silver nanoparticle functionalized glass fibers for combined surface-enhanced Raman scattering spectroscopy (SERS)/surface-assisted laser desorption/ionization (SALDI) mass spectrometry via plasmonic/thermal hot spots. *Analyst* **2016**, *141*, 5835–5841.
[81] Deng, D.; Lin, Q. Y.; Li, H.; Huang, Z. P.; Kuang, Y. Y.; Chen, H.; Kong, J. L. Rapid detection of malachite green residues in fish using a surface-enhanced Raman scattering-active glass fiber paper prepared by *in situ* reduction method. *Talanta* **2019**, *200*, 272–278.
[82] Xu, J. T.; Li, X. T.; Wang, Y. X.; Guo, R. H.; Shang, S. M.; Jiang, S. X. Flexible and reusable cap-like thin Fe_2O_3 film for SERS applications. *Nano Res.* **2019**, *12*, 381–388.
[83] Ge, F. Y.; Chen, Y. M.; Liu, A. R.; Guang, S. Y.; Cai, Z. S. Flexible and recyclable SERS substrate fabricated by decorated TiO_2 film with Ag NPs on the cotton fabric. *Cellulose* **2019**, *26*, 2689–2697.
[84] Gong, Z. J.; Du, H. J.; Cheng, F. S.; Wang, C.; Wang, C. C.; Fan, M. K. Fabrication of SERS swab for direct detection of trace explosives in fingerprints. *ACS Appl. Mater. Interfaces* **2014**, *6*, 21931–21937.
[85] Gao, W.; Xu, J. T.; Cheng, C.; Qiu, S.; Jiang, S. X. Rapid and highly sensitive SERS detection of fungicide based on flexible "wash free" metallic textile. *Appl. Surf. Sci.* **2020**, *512*, 144693.
[86] Cheng, D. S.; He, M. T.; Ran, J. H.; Cai, G. M.; Wu, J. H.; Wang, X. Depositing a flexible substrate of triangular silver nanoplates onto cotton fabrics for sensitive SERS detection. *Sens. Actuators B:Chem.* **2018**, *270*, 508–517.
[87] Huang, J. A.; Zhang, Y. L.; Zhao, Y. Q.; Zhang, X. L.; Sun, M. L.; Zhang, W. J. Superhydrophobic SERS chip based on a Ag coated natural taro-leaf. *Nanoscale* **2016**, *8*, 11487–11493.
[88] Sharma, V.; Balaji, R.; Walia, R.; Krishnan, V. Au nanoparticle aggregates assembled on 3D mirror-like configuration using *Canna generalis* leaves for SERS applications. *Colloids Interface Sci. Commun.* **2017**, *18*, 9–12.
[89] Ding, Q.; Kang, Z. W.; He, X. S.; Wang, M. G.; Lin, M. S.; Lin, H. T.; Yang, D. P. Eggshell membrane-templated gold nanoparticles as a flexible SERS substrate for detection of thiabendazole. *Microchim. Acta* **2019**, *186*, 453.
[90] Wang, M. L.; Shi, G. C.; Zhu, Y. Y.; Wang, Y. H.; Ma, W. L. Au-decorated dragonfly wing bioscaffold arrays as flexible surface-enhanced Raman scattering (SERS) substrate for simultaneous determination of pesticide residues. *Nanomaterials* **2018**, *8*, 289.
[91] Zhang, M. F.; Meng, J. T.; Wang, D. P.; Tang, Q.; Chen, T.; Rong, S. Z.; Liu, J. Q.; Wu, Y. C. Biomimetic synthesis of hierarchical 3D Ag butterfly wing scale arrays/graphene composites as ultrasensitive SERS substrates for efficient trace chemical detection. *J. Mater. Chem. C* **2018**, *6*, 1933–1943.
[92] Zhao, N.; Li, H. F.; Tian, C. W.; Xie, Y. R.; Feng, Z. B.; Wang, Z. L.; Yan, X. L.; Wang, W. J.; Yu, H. S. Bioscaffold arrays decorated with Ag nanoparticles as a SERS substrate for direct detection of

melamine in infant formula. *RSC Adv.* **2019**, *9*, 21771–21776.
[93] Chou, S. Y.; Yu, C. C.; Yen, Y. T.; Lin, K. T.; Chen, H. L.; Su, W. F. Romantic story or Raman scattering? Rose petals as ecofriendly, low-cost substrates for ultrasensitive surface-enhanced Raman scattering. *Anal. Chem.* **2015**, *87*, 6017–6024.
[94] Shi, G. C.; Wang, M. L.; Zhu, Y. Y.; Shen, L.; Ma, W. L.; Wang, Y. H.; Li, R. F. Dragonfly wing decorated by gold nanoislands as flexible and stable substrates for surface-enhanced Raman scattering (SERS). *Sci. Rep.* **2018**, *8*, 6916.
[95] Godoy, N. V.; García-Lojo, D.; Sigoli, F. A.; Pérez-Juste, J.; Pastoriza-Santos, I.; Mazali, I. O. Ultrasensitive inkjet-printed based SERS sensor combining a high-performance gold nanosphere ink and hydrophobic paper. *Sens. Actuators B:Chem.* **2020**, *320*, 128412.
[96] Xu, M.; Tu, G. P.; Ji, M. W.; Wan, X. D.; Liu, J. J.; Liu, J.; Rong, H. P.; Yang, Y. L.; Wang, C.; Zhang, J. T. Vacuum-tuned-atmosphere induced assembly of Au@Ag core/shell nanocubes into multi-dimensional superstructures and the ultrasensitive IAPP proteins SERS detection. *Nano Res.* **2019**, *12*, 1375–1379.
[97] Tong, J. H.; Xu, Z. X.; Bian, Y. X.; Niu, Y. T.; Zhang, Y. Y.; Wang, Z. N. Flexible and smart fibers decorated with Ag nanoflowers for highly active surface-enhanced Raman scattering detection. *J. Raman Spectrosc.* **2019**, *50*, 1468–1476.
[98] Park, S.; Lee, J.; Ko, H. Transparent and flexible surface-enhanced Raman scattering (SERS) sensors based on gold nanostar arrays embedded in silicon rubber film. *ACS Appl. Mater. Interfaces* **2017**, *9*, 44088–44095.
[99] Aparicio-Martínez, E.; Estrada-Moreno, I. A.; Dominguez, R. B. Fabrication of flexible composite of laser reduced graphene@Ag dendrites as active material for surface enhanced Raman spectroscopy. *Mater. Lett.* **2020**, *277*, 128380.
[100] Tian, Y. R.; Liu, H. M.; Chen, Y.; Zhou, C. L.; Jiang, Y.; Gu, C. J.; Jiang, T.; Zhou, J. Seedless one-spot synthesis of 3D and 2D Ag nanoflowers for multiple phase SERS-based molecule detection. *Sens. Actuators B:Chem.* **2019**, *301*, 127142.
[101] Gao, R. K.; Qian, H. Y.; Weng, C. G.; Wang, X. L.; Xie, C.; Guo, K.; Zhang, S. S.; Xuan, S. H.; Guo, Z. Y.; Luo, L. B. A SERS stamp: Multiscale coupling effect of silver nanoparticles and highly ordered nano-micro hierarchical substrates for ultrasensitive explosive detection. *Sens. Actuators B:Chem.* **2020**, *321*, 128543.
[102] Ding, S. Y.; You, E. M.; Tian, Z. Q.; Moskovits, M. Electromagnetic theories of surface-enhanced Raman spectroscopy. *Chem. Soc. Rev.* **2017**, *46*, 4042–4076.
[103] Cao, Y. Q.; Zhang, J. W.; Yang, Y.; Huang, Z. R.; Long, N. V.; Fu, C. L. Engineering of SERS substrates based on noble metal nanomaterials for chemical and biomedical applications. *Appl. Spectrosc. Rev.* **2015**, *50*, 499–525.
[104] Zhang, Y.; Yang, C. L.; Xue, B.; Peng, Z. H.; Cao, Z. L.; Mu, Q. Q.; Xuan, L. Highly effective and chemically stable surface enhanced Raman scattering substrates with flower-like 3D Ag-Au hetero-nanostructures. *Sci. Rep.* **2018**, *8*, 898.
[105] Wang, K. Q.; Sun, D. W.; Pu, H. B.; Wei, Q. Y.; Huang, L. J. Stable, flexible, and high-performance SERS chip enabled by a ternary film-packaged plasmonic nanoparticle array. *ACS Appl. Mater. Interfaces* **2019**, *11*, 29177–29186.
[106] Nganou, C.; Carrier, A. J.; Yang, D. C.; Chen, Y. L.; Yu, N. Z.; Richards, D. D.; Bennett, C.; Oakes, K. D.; Zhang, X. Ultrasensitive and remote SERS enabled by oxygen-free integrated plasmonic field transmission. *Cell Rep. Phys. Sci.* **2020**, *1*, 100189.
[107] Yan, X. Y.; Wang, M. L.; Sun, X.; Wang, Y. H.; Shi, G. C.; Ma, W. L.; Hou, P. Sandwich-like Ag@Cu@CW SERS substrate with tunable nanogaps and component based on the Plasmonic nanonodule structures for sensitive detection crystal violet and 4-aminothiophenol. *Appl. Surf. Sci.* **2019**, *479*, 879–886.
[108] Encina, E. R.; Coronado, E. A. Near field enhancement in Ag Au nanospheres heterodimers. *J. Phys. Chem. C* **2011**, *115*, 15908–15914.
[109] Yan, X. Y.; Wang, Y. H.; Shi, G. C.; Wang, M. L.; Zhang, J. Z.; Sun, X.; Xu, H. J. Flower-like Cu nanoislands decorated onto the cicada wing as SERS substrates for the rapid detection of crystal violet. *Optik* **2018**, *172*, 812–821.
[110] Zhao, X. H.; Deng, M.; Rao, G. F.; Yan, Y. C.; Wu, C. Y.; Jiao, Y.; Deng, A. Q.; Yan, C. Y.; Huang, J. W.; Wu, S. H. et al. High-performance SERS substrate based on hierarchical 3D Cu nanocrystals with efficient morphology control. *Small* **2018**, *14*, 1802477.
[111] Chen, L. Y.; Yu, J. S.; Fujita, T.; Chen, M. W. Nanoporous copper with tunable nanoporosity for SERS applications. *Adv. Funct. Mater.* **2009**, *19*, 1221–1226.
[112] Chen, K.; Zhang, X.; Zhang, Y. L.; Lei, D. Y.; Li, H. T.; Williams, T.; MacFarlane, D. R. Highly ordered Ag/Cu hybrid nanostructure arrays for ultrasensitive surface-enhanced Raman spectroscopy. *Adv. Mater. Interfaces* **2016**, *3*, 1600115.
[113] Zheng, Z. H.; Cong, S.; Gong, W. B.; Xuan, J. N.; Li, G. H.; Lu, W. B.; Geng, F. X.; Zhao, Z. G. Semiconductor SERS enhancement enabled by oxygen incorporation. *Nat. Commun.* **2017**, *8*, 1993.
[114] Wang, X. T.; Guo, L. SERS activity of semiconductors: Crystalline and amorphous nanomaterials. *Angew. Chem., Int. Ed.* **2020**, *59*, 4231–4239.
[115] Hou, X. Y.; Fan, X. C.; Wei, P. H.; Qiu, T. Planar transition metal oxides SERS chips: A general strategy. *J. Mater. Chem. C* **2019**, *7*, 11134–11141.
[116] Zhang, N.; Tong, L. M.; Zhang, J. Graphene-based enhanced Raman scattering toward analytical applications. *Chem. Mater.* **2016**, *28*, 6426–6435.
[117] Pan, X.; Li, L. H.; Lin, H. D.; Tan, J. Y.; Wang, H. T.; Liao, M. L.; Chen, C. J.; Shan, B. B.; Chen, Y. F.; Li, M. A graphene oxide-gold nanostar hybrid based-paper biosensor for label-free SERS detection of serum bilirubin for diagnosis of jaundice. *Biosens. Bioelectron.* **2019**, *145*, 111713.
[118] Lv, P.; Chen, Z. D.; Ma, Z. C.; Mao, J. W.; Han, B.; Han, D. D.; Zhang, Y. L. Ag nanoparticle ink coupled with graphene oxide cellulose paper: A flexible and tunable SERS sensing platform. *Opt. Lett.* **2020**, *45*, 4208–4211.
[119] Liang, X.; Liang, B. L.; Pan, Z. H.; Lang, X. F.; Zhang, Y. G.; Wang, G. S.; Yin, P. G.; Guo, L. Tuning plasmonic and chemical enhancement for SERS detection on graphene-based Au hybrids. *Nanoscale* **2015**, *7*, 20188–20196.
[120] Naqvi, T. K.; Srivastava, A. K.; Kulkarni, M. M.; Siddiqui, A. M.; Dwivedi, P. K. Silver nanoparticles decorated reduced graphene oxide (rGO) SERS sensor for multiple analytes. *Appl. Surf. Sci.* **2019**, *478*, 887–895.
[121] Nair, A. K.; Bhavitha, K. B.; Perumbilavil, S.; Sankar, P.; Rouxel, D.; Kala, M. S.; Thomas, S.; Kalarikkal, N. Multifunctional nitrogen sulfur co-doped reduced graphene oxide-Ag nano hybrids (sphere, cube and wire) for nonlinear optical and SERS applications. *Carbon* **2018**, *132*, 380–393.
[122] Zhang, X. G.; Dai, Z. G.; Si, S. Y.; Zhang, X. L.; Wu, W.; Deng, H. B.; Wang, F. B.; Xiao, X. H.; Jiang, C. Z. Ultrasensitive SERS substrate integrated with uniform subnanometer scale "Hot Spots" created by a graphene spacer for the detection of mercury ions. *Small* **2017**, *13*, 1603347.
[123] Ponlamuangdee, K.; Hornyak, G. L.; Bora, T.; Bamrungsap, S. Graphene oxide/gold nanorod plasmonic paper—A simple and cost-effective SERS substrate for anticancer drug analysis. *New J. Chem.* **2020**, *44*, 14087–14094.
[124] Xin, W. B.; Yang, J. M.; Li, C.; Goorsky, M. S.; Carlson, L.; De Rosa, I. M. Novel strategy for one-pot synthesis of gold nanoplates on carbon nanotube sheet as an effective flexible SERS substrate. *ACS Appl. Mater. Interfaces* **2017**, *9*, 6246–6254.
[125] Fortuni, B.; Fujita, Y.; Ricci, M.; Inose, T.; Aubert, R.; Lu, G.; Hutchison, J. A.; Hofkens, J.; Latterini, L.; Uji-i, H. A novel method for *in situ* synthesis of SERS-active gold nanostars on polydimethylsiloxane film. *Chem. Commun.* **2017**, *53*, 5121–5124.
[126] Zong, C. H.; Ge, M. Y.; Pan, H.; Wang, J.; Nie, X. M.; Zhang, Q. Q.; Zhao, W. F.; Liu, X. J.; Yu, Y. *In situ* synthesis of low-cost and large-scale flexible metal nanoparticle-polymer composite films as highly sensitive SERS substrates for surface trace analysis. *RSC Adv.* **2019**, *9*, 2857–2864.
[127] Fortuni, B.; Inose, T.; Uezono, S.; Toyouchi, S.; Umemoto, K.;

Sekine, S.; Fujita, Y.; Ricci, M.; Lu, G.; Masuhara, A. et al. *In situ* synthesis of Au-shelled Ag nanoparticles on PDMS for flexible, long-life, and broad spectrum-sensitive SERS substrates. *Chem. Commun.* **2017**, *53*, 11298–11301.

[128] Chen, D. Z.; Zhang, L.; Ning, P.; Yuan, H. Z.; Zhang, Y.; Zhang, M.; Fu, T.; He, X. H. *In-situ* growth of gold nanoparticles on electrospun flexible multilayered PVDF nanofibers for SERS sensing of molecules and bacteria. *Nano Res.* **2021**, *14*, 4885–4893.

[129] Liu, X. F.; Ma, J. M.; Jiang, P. F.; Shen, J. L.; Wang, R. W.; Wang, Y.; Tu, G. L. Large-scale flexible surface-enhanced Raman scattering (SERS) sensors with high stability and signal homogeneity. *ACS Appl. Mater. Interfaces* **2020**, *12*, 45332–45341.

[130] Jia, K.; Xie, J. N.; He, X. H.; Zhang, D. W.; Hou, B. S.; Li, X. S.; Zhou, X.; Hong, Y.; Liu, X. B. Polymeric micro-reactors mediated synthesis and assembly of Ag nanoparticles into cube-like superparticles for SERS application. *Chem. Eng. J.* **2020**, *395*, 125123.

[131] Zhang, L. L.; Li, X. D.; Liu, W. H.; Hao, R.; Jia, H. R.; Dai, Y. Z.; Amin, M. U.; You, H. J.; Li, T.; Fang, J. X. Highly active Au NP microarray films for direct SERS detection. *J. Mater. Chem. C* **2019**, *7*, 15259–15268.

[132] George, J. E.; Unnikrishnan, V. K.; Mathur, D.; Chidangil, S.; George, S. D. Flexible superhydrophobic SERS substrates fabricated by *in situ* reduction of Ag on femtosecond laser-written hierarchical surfaces. *Sens. Actuators B:Chem.* **2018**, *272*, 485–493.

[133] Yang, F.; Chen, L.; Li, D. Y.; Xu, Y.; Li, S. B.; Wang, L. Printer-assisted array flexible surface-enhanced Raman spectroscopy chip preparation for rapid and label-free detection of bacteria. *J. Raman Spectrosc.* **2020**, *51*, 932–940.

[134] Fu, F. Y.; Yang, B. B.; Hu, X. M.; Tang, H. Y.; Zhang, Y. P.; Xu, X. Y.; Zhang, Y. Y.; Touhid, S. S. B.; Liu, X. D.; Zhu, Y. F. et al. Biomimetic synthesis of 3D Au-decorated chitosan nanocomposite for sensitive and reliable SERS detection. *Chem. Eng. J.* **2020**, *392*, 123693.

[135] Cai, J.; Wang, Z. H.; Wang, M. J.; Zhang, D. Y. Au nanoparticle-grafted hierarchical pillars array replicated from diatom as reliable SERS substrates. *Appl. Surf. Sci.* **2021**, *541*, 148374.

[136] Nowicka, A. B.; Czaplicka, M.; Kowalska, A. A.; Szymborski, T.; Kamińska, A. Flexible PET/ITO/Ag SERS platform for label-free detection of pesticides. *Biosensors* **2019**, *9*, 111.

[137] Zhang, C. P.; Yi, P. Y.; Peng, L. F.; Lai, X. M.; Chen, J.; Huang, M. Z.; Ni, J. Continuous fabrication of nanostructure arrays for flexible surface enhanced Raman scattering substrate. *Sci. Rep.* **2017**, *7*, 39814.

[138] Kralchevsky, P. A.; Nagayama, K. Capillary forces between colloidal particles. *Langmuir* **1994**, *10*, 23–36.

[139] Zhou, N. N.; Meng, G. W.; Huang, Z. L.; Ke, Y.; Zhou, Q. T.; Hu, X. Y. A flexible transparent Ag-NC@PE film as a cut-and-paste SERS substrate for rapid *in situ* detection of organic pollutants. *Analyst* **2016**, *141*, 5864–5869.

[140] Alyami, A.; Quinn, A. J.; Iacopino, D. Flexible and transparent surface enhanced Raman scattering (SERS)-active Ag NPs/PDMS composites for *in-situ* detection of food contaminants. *Talanta* **2019**, *201*, 58–64.

[141] Wu, P.; Zhong, L. B.; Liu, Q.; Zhou, X.; Zheng, Y. M. Polymer induced one-step interfacial self-assembly method for the fabrication of flexible, robust and free-standing SERS substrates for rapid on-site detection of pesticide residues. *Nanoscale* **2019**, *11*, 12829–12836.

[142] Marta, S. D.; Novara, C.; Giorgis, F.; Bonifacio, A.; Sergo, V. Optimization and characterization of paper-made surface enhanced Raman scattering (SERS) substrates with Au and Ag NPs for quantitative analysis. *Materials* **2017**, *10*, 1365.

[143] Villa, J. E. L.; Quiñones, N. R.; Fantinatti-Garboggini, F.; Poppi, R. J. Fast discrimination of bacteria using a filter paper-based SERS platform and PLS-DA with uncertainty estimation. *Anal. Bioanal. Chem.* **2019**, *411*, 705–713.

[144] Deegan, R. D.; Bakajin, O.; Dupont, T. F.; Huber, G.; Nagel, S. R.; Witten, T. A. Capillary flow as the cause of ring stains from dried liquid drops. *Nature* **1997**, *389*, 827–829.

[145] Liu, Y.; Zhou, F.; Wang, H. C.; Huang, X. Y.; Ling, D. X. Micro-coffee-ring-patterned fiber SERS probes and their *in situ* detection application in complex liquid environments. *Sens. Actuators B:Chem.* **2019**, *299*, 126990.

[146] Wu, W.; Liu, L.; Dai, Z. G.; Liu, J. H.; Yang, S. L.; Zhou, L.; Xiao, X. H.; Jiang, C. Z.; Roy, V. A. L. Low-cost, disposable, flexible and highly reproducible screen printed SERS substrates for the detection of various chemicals. *Sci. Rep.* **2015**, *5*, 10208.

[147] Weng, G. J.; Yang, Y.; Zhao, J.; Li, J. J.; Zhu, J.; Zhao, J. W. Improving the SERS enhancement and reproducibility of inkjet-printed Au NP paper substrates by second growth of Ag nanoparticles. *Mater. Chem. Phys.* **2020**, *253*, 123416.

[148] Liao, W. J.; Roy, P. K.; Chattopadhyay, S. An ink-jet printed, surface enhanced Raman scattering paper for food screening. *RSC Adv.* **2014**, *4*, 40487–40493.

[149] Sykam, N.; Jayram, N. D.; Rao, G. M. Exfoliation of graphite as flexible SERS substrate with high dye adsorption capacity for Rhodamine 6G. *Appl. Surf. Sci.* **2019**, *471*, 375–386.

[150] Purwidyantri, A.; Hsu, C. H.; Yang, C. M.; Prabowo, B. A.; Tian, Y. C.; Lai, C. S. Plasmonic nanomaterial structuring for SERS enhancement. *RSC Adv.* **2019**, *9*, 4982–4992.

[151] Xu, D. P.; Kang, W. G.; Zhang, S.; Yang, W.; Jiang, H. Z.; Lei, Y. P.; Chen, J. Fractal theory and controllable preparation of centimeter level silver nanowire arrays and their application in melamine detection as SERS substrates. *Spectrochim. Acta Part A:Mol. Biomol. Spectrosc.* **2019**, *221*, 117184.

[152] Liu, Y.; Kim, M.; Cho, S. H.; Jung, Y. S. Vertically aligned nanostructures for a reliable and ultrasensitive SERS-active platform: Fabrication and engineering strategies. *Nano Today* **2021**, *37*, 101063.

[153] Zang, S. Y.; Liu, H.; Wang, Q.; Yang, J. W.; Pang, Z. Q.; Liu, K.; Cai, S. W.; Ren, X. M. Facile fabrication of Au nanoworms covered polyethylene terephthalate (PET) film: Towards flexible SERS substrates. *Mater. Lett.* **2021**, *294*, 129643.

[154] Guo, X. F.; Wang, D. P.; Khan, R. Nafion stabilized Ag nanopillar arrays as a flexible SERS substrate for trace chemical detection. *Mater. Chem. Phys.* **2020**, *252*, 123291.

[155] Wei, W.; Du, Y. X.; Zhang, L. M.; Yang, Y.; Gao, Y. F. Improving SERS hot spots for on-site pesticide detection by combining silver nanoparticles with nanowires. *J. Mater. Chem. C* **2018**, *6*, 8793–8803.

[156] Zhao, P. N.; Liu, H. Y.; Zhang, L. N.; Zhu, P. H.; Ge, S. G.; Yu, J. H. Paper-based SERS sensing platform based on 3D silver dendrites and molecularly imprinted identifier sandwich hybrid for neonicotinoid quantification. *ACS Appl. Mater. Interfaces* **2020**, *12*, 8845–8854.

[157] He, X. C.; Yang, S. J.; Xu, T. L.; Song, Y. C.; Zhang, X. J. Microdroplet-captured tapes for rapid sampling and SERS detection of food contaminants. *Biosens. Bioelectron.* **2020**, *152*, 112013.

[158] Liu, H. Y.; Zhao, P. N.; Wang, Y.; Li, S. S.; Zhang, L. N.; Zhang, Y.; Ge, S. G.; Yu, J. H. Paper-based sandwich type SERS sensor based on silver nanoparticles and biomimetic recognizer. *Sens. Actuators B:Chem.* **2020**, *313*, 127989.

[159] Cheung, M.; Lee, W. W. Y.; McCracken, J. N.; Larmour, I. A.; Brennan, S.; Bell, S. E. J. Raman analysis of dilute aqueous samples by localized evaporation of submicroliter droplets on the tips of superhydrophobic copper wires. *Anal. Chem.* **2016**, *88*, 4541–4547.

[160] Lu, S. C.; You, T. T.; Yang, N.; Gao, Y. K.; Yin, P. G. Flexible SERS substrate based on Ag nanodendrite-coated carbon fiber cloth: Simultaneous detection for multiple pesticides in liquid droplet. *Anal. Bioanal. Chem.* **2020**, *412*, 1159–1167.

[161] Sun, Y. N.; Chen, X. D.; Zheng, Y. X.; Song, Y. H.; Zhang, H. R.; Zhang, S. S. Surface-enhanced Raman scattering trace-detection platform based on continuous-rolling-assisted evaporation on superhydrophobic surfaces. *ACS Appl. Nano Mater.* **2020**, *3*, 4767–4776.

[162] Villa, J. E. L.; Afonso, M. A. S.; Dos Santos, D. P.; Mercadal, P. A.; Coronado, E. A.; Poppi, R. J. Colloidal gold clusters formation and chemometrics for direct SERS determination of bioanalytes in complex media. *Spectrochim. Acta Part A:Mol. Biomol. Spectrosc.* **2020**, *224*, 117380.

[163] Pérez-Jiménez, A. I.; Lyu, D. Y.; Lu, Z. X.; Liu, G. K.; Ren, B. Surface-enhanced Raman spectroscopy: Benefits, trade-offs and future developments. *Chem. Sci.* **2020**, *11*, 4563–4577.
[164] Ye, D. D.; Lei, X. J.; Li, T.; Cheng, Q. Y.; Chang, C. Y.; Hu, L. B.; Zhang, L. N. Ultrahigh tough, super clear, and highly anisotropic nanofiber-structured regenerated cellulose films. *ACS Nano* **2019**, *13*, 4843–4853.
[165] Hu, X. M.; Yang, B. B.; Wen, X. D.; Su, J. N.; Jia, B. Q.; Fu, F. Y.; Zhang, Y. Y.; Yu, Q. L.; Liu, X. D. One-pot synthesis of a three-dimensional Au-decorated cellulose nanocomposite as a surface-enhanced Raman scattering sensor for selective detection and *in situ* monitoring. *ACS Sustainable Chem. Eng.* **2021**, *9*, 3324–3336.
[166] Wang, X. J.; Xu, Q. L.; Hu, X. Y.; Han, F. M.; Zhu, C. H. Silver-nanoparticles/graphene hybrids for effective enrichment and sensitive SERS detection of polycyclic aromatic hydrocarbons. *Spectrochim. Acta Part A:Mol. Biomol. Spectrosc.* **2020**, *228*, 117783.
[167] Li, J. Y.; Heng, H.; Lv, J. L.; Jiang, T. T.; Wang, Z. Y.; Dai, Z. H. Graphene oxide-assisted and DNA-modulated SERS of AuCu alloy for the fabrication of apurinic/apyrimidinic endonuclease 1 biosensor. *Small* **2019**, *15*, 1901506.
[168] Shafer-Peltier, K. E.; Haynes, C. L.; Glucksberg, M. R.; Van Duyne, R. P. Toward a glucose biosensor based on surface-enhanced Raman scattering. *J. Am. Chem. Soc.* **2003**, *125*, 588–593.
[169] Yun, B. J.; Koh, W. G. Highly-sensitive SERS-based immunoassay platform prepared on silver nanoparticle-decorated electrospun polymeric fibers. *J. Ind. Eng. Chem.* **2020**, *82*, 341–348.
[170] Carneiro, M. C. C. G.; Sousa-Castillo, A.; Correa-Duarte, M. A.; Sales, M. G. F. Dual biorecognition by combining molecularly-imprinted polymer and antibody in SERS detection. Application to carcinoembryonic antigen. *Biosens. Bioelectron.* **2019**, *146*, 111761.
[171] Khlebtsov, B. N.; Bratashov, D. N.; Byzova, N. A.; Dzantiev, B. B.; Khlebtsov, N. G. SERS-based lateral flow immunoassay of troponin I by using gap-enhanced Raman tags. *Nano Res.* **2019**, *12*, 413–420.
[172] Safar, W.; Tatar, A. S.; Leray, A.; Potara, M.; Liu, Q. Q.; Edely, M.; Djaker, N.; Spadavecchia, J.; Fu, W. L.; Derouich, S. G. et al. New insight into the aptamer conformation and aptamer/protein interaction by surface-enhanced Raman scattering and multivariate statistical analysis. *Nanoscale* **2021**, *13*, 12443–12453.
[173] Fan, W. L.; Yang, S. W.; Zhang, Y. Z.; Huang, B.; Gong, Z. J.; Wang, D. M.; Fan, M. K. Multifunctional flexible SERS sensor on a fixate gel pad: Capturing, derivation, and selective picogram indirect detection of explosive 2, 2′, 4, 4′, 6, 6′-hexanitrostilbene. *ACS Sens.* **2020**, *5*, 3599–3606.
[174] Reokrungruang, P.; Chatnuntawech, I.; Dharakul, T.; Bamrungsap, S. A simple paper-based surface enhanced Raman scattering (SERS) platform and magnetic separation for cancer screening. *Sens. Actuators B:Chem.* **2019**, *285*, 462–469.
[175] Blanco-Covián, L.; Montes-García, V.; Girard, A.; Fernández-Abedul, M. T.; Pérez-Juste, J.; Pastoriza-Santos, I.; Faulds, K.; Graham, D.; Blanco-López, M. C. Au@Ag SERRS tags coupled to a lateral flow immunoassay for the sensitive detection of pneumolysin. *Nanoscale* **2017**, *9*, 2051–2058.
[176] Lim, W. Y.; Goh, C. H.; Thevarajah, T. M.; Goh, B. T.; Khor, S. M. Using SERS-based microfluidic paper-based device (μPAD) for calibration-free quantitative measurement of AMI cardiac biomarkers. *Biosens. Bioelectron.* **2020**, *147*, 111792.
[177] Liu, X. X.; Yang, X. S.; Li, K.; Liu, H. F.; Xiao, R.; Wang, W. Y.; Wang, C. W.; Wang, S. Q. Fe_3O_4@Au SERS tags-based lateral flow assay for simultaneous detection of serum amyloid A and C-reactive protein in unprocessed blood sample. *Sens. Actuators B:Chem.* **2020**, *320*, 128350.
[178] Lu, T.; Wang, L. P.; Xia, Y. H.; Jin, Y.; Zhang, L. Y.; Du, S. H. A multimer-based SERS aptasensor for highly sensitive and homogeneous assay of carcinoembryonic antigens. *Analyst* **2021**, *146*, 3016–3024.
[179] Yang, M. X.; Liu, G. K.; Mehedi, H. M.; Ouyang, Q.; Chen, Q. S. A universal SERS aptasensor based on DTNB labeled GNTs/Ag core–shell nanotriangle and CS-Fe_3O_4 magnetic-bead trace detection of Aflatoxin B1. *Anal. Chim. Acta* **2017**, *986*, 122–130.
[180] Dunn, M. R.; McCloskey, C. M.; Buckley, P.; Rhea, K.; Chaput, J. C. Generating biologically stable TNA aptamers that function with high affinity and thermal stability. *J. Am. Chem. Soc.* **2020**, *142*, 7721–7724.
[181] Zhu, L. J.; Li, S. T.; Shao, X. L.; Feng, Y. X.; Xie, P. Y.; Luo, Y. B.; Huang, K. L.; Xu, W. T. Colorimetric detection and typing of *E. coli* lipopolysaccharides based on a dual aptamer-functionalized gold nanoparticle probe. *Microchim. Acta* **2019**, *186*, 111.
[182] Alizadeh, N.; Memar, M. Y.; Moaddab, S. R.; Kafil, H. S. Aptamer-assisted novel technologies for detecting bacterial pathogens. *Biomed. Pharmacother.* **2017**, *93*, 737–745.
[183] Zhu, A. F.; Ali, S.; Xu, Y.; Ouyang, Q.; Chen, Q. S. A SERS aptasensor based on AuNPs functionalized PDMS film for selective and sensitive detection of *Staphylococcus aureus*. *Biosens. Bioelectron.* **2021**, *172*, 112806.
[184] Haupt, K.; Rangel, P. X. M.; Bui, B. T. S. Molecularly imprinted polymers: Antibody mimics for bioimaging and therapy. *Chem. Rev.* **2020**, *120*, 9554–9582.
[185] Til, R. F.; Alizadeh-Khaledabad, M.; Mohammadi, R.; Pirsa, S.; Wilson, L. D. Molecular imprinted polymers for the controlled uptake of sinapic acid from aqueous media. *Food Funct.* **2020**, *11*, 895–906.
[186] Marcelo, G.; Ferreira, I. C.; Viveiros, R.; Casimiro, T. Development of itaconic acid-based molecular imprinted polymers using supercritical fluid technology for pH-triggered drug delivery. *Int. J. Pharmaceut.* **2018**, *542*, 125–131.
[187] Li, Y. T.; Yang, Y. Y.; Sun, Y. X.; Cao, Y.; Huang, Y. S.; Han, S. Electrochemical fabrication of reduced MoS_2-based portable molecular imprinting nanoprobe for selective SERS determination of theophylline. *Microchim. Acta* **2020**, *187*, 203.
[188] Guo, X. T.; Li, J. H.; Arabi, M.; Wang, X. Y.; Wang, Y. Q.; Chen, L. X. Molecular-imprinting-based surface-enhanced Raman scattering sensors. *ACS Sens.* **2020**, *5*, 601–619.
[189] Prakash, J. Fundamentals and applications of recyclable SERS substrates. *Int. Rev. Phys. Chem.* **2019**, *38*, 201–242.
[190] Pal, A. K.; Chandra, G. K.; Umapathy, S.; Mohan, D. B. Ultra-sensitive, reusable, and superhydrophobic Ag/ZnO/Ag 3D hybrid surface enhanced Raman scattering substrate for hemoglobin detection. *J. Appl. Phys.* **2020**, *127*, 164501.
[191] Li, C. C.; Huang, Y. M.; Li, X. Y.; Zhang, Y. R.; Chen, Q. L.; Ye, Z. W.; Alqarni, Z.; Bell, S. E. J.; Xu, Y. K. Towards practical and sustainable SERS: A review of recent developments in the construction of multifunctional enhancing substrates. *J. Mater. Chem. C* **2021**, *9*, 11517–11552.
[192] Sakir, M.; Salem, S.; Sanduvac, S. T.; Sahmetlioglu, E.; Sarp, G.; Onses, M. S.; Yilmaz, E. Photocatalytic green fabrication of Au nanoparticles on ZnO nanorods modified membrane as flexible and photocatalytic active reusable SERS substrates. *Colloids Surf. A:Physicochem. Eng. Aspects* **2020**, *585*, 124088.
[193] Li, J. T.; Wu, N. Q. Semiconductor-based photocatalysts and photoelectrochemical cells for solar fuel generation: A review. *Catal. Sci. Technol.* **2015**, *5*, 1360–1384.
[194] Khan, S. A.; Arshad, Z.; Shahid, S.; Arshad, I.; Rizwan, K.; Sher, M.; Fatima, U. Synthesis of TiO_2/graphene oxide nanocomposites for their enhanced photocatalytic activity against methylene blue dye and ciprofloxacin. *Compos. Part B:Eng.* **2019**, *175*, 107120.
[195] Xiong, L. Q.; Tang, J. W. Strategies and challenges on selectivity of photocatalytic oxidation of organic substances. *Adv. Energy Mater.* **2021**, *11*, 2003216.
[196] Kou, J. H.; Lu, C. H.; Wang, J.; Chen, Y. K.; Xu, Z. Z.; Varma, R. S. Selectivity enhancement in heterogeneous photocatalytic transformations. *Chem. Rev.* **2017**, *117*, 1445–1514.
[197] Zhu, T.; Wang, H.; Zang, L. B.; Jin, S. L.; Guo, S.; Park, E.; Mao, Z.; Jung, Y. M. Flexible and reusable Ag coated TiO_2 nanotube arrays for highly sensitive SERS detection of formaldehyde. *Molecules* **2020**, *25*, 1199.
[198] Hao, Q.; Li, M. Z.; Wang, J. W.; Fan, X. C.; Jiang, J.; Wang, X. X.; Zhu, M. S.; Qiu, T.; Ma, L. B.; Chu, P. K. et al. Flexible surface-

enhanced Raman scattering chip: A universal platform for real-time interfacial molecular analysis with femtomolar sensitivity. *ACS Appl. Mater. Interfaces* **2020**, *12*, 54174–54180.

[199] Yang, J.; Xu, J. T.; Bian, X. Y.; Pu, Y.; Chiu, K. L.; Miao, D. G.; Jiang, S. X. Flexible and reusable SERS substrate for rapid conformal detection of residue on irregular surface. *Cellulose* **2021**, *28*, 921–936.

[200] Bamrungsap, S.; Treetong, A.; Apiwat, C.; Wuttikhun, T.; Dharakul, T. SERS-fluorescence dual mode nanotags for cervical cancer detection using aptamers conjugated to gold–silver nanorods. *Microchim. Acta* **2016**, *183*, 249–256.

[201] Villa, J. E. L.; Poppi, R. J. A portable SERS method for the determination of uric acid using a paper-based substrate and multivariate curve resolution. *Analyst* **2016**, *141*, 1966–1972.

[202] Tang, S. Q.; Liu, H. M.; Tian, Y. R.; Chen, D.; Gu, C. J.; Wei, G. D.; Jiang, T.; Zhou, J. Surface-enhanced Raman scattering-based lateral flow immunoassay mediated by hydrophilic–hydrophobic Ag-modified PMMA substrate. *Spectrochim. Acta Part A:Mol. Biomol. Spectrosc.* **2021**, *262*, 120092.

[203] Crawford, A. C.; Laurentius, L. B.; Mulvihill, T. S.; Granger, J. H.; Spencer, J. S.; Chatterjee, D.; Hanson, K. E.; Porter, M. D. Detection of the tuberculosis antigenic marker mannose-capped lipoarabinomannan in pretreated serum by surface-enhanced Raman scattering. *Analyst* **2017**, *142*, 186–196.

[204] Kim, W.; Lee, S. H.; Kim, J. H.; Ahn, Y. J.; Kim, Y. H.; Yu, J. S.; Choi, S. Paper-based surface-enhanced Raman spectroscopy for diagnosing prenatal diseases in women. *ACS Nano* **2018**, *12*, 7100–7108.

[205] Narasimhan, V.; Siddique, R. H.; Park, H.; Choo, H. Bioinspired disordered flexible metasurfaces for human tear analysis using broadband surface-enhanced Raman scattering. *ACS Omega* **2020**, *5*, 12915–12922.

[206] Wang, Y. L.; Zhao, C.; Wang, J. J.; Luo, X.; Xie, L. J.; Zhan, S. J.; Kim, J.; Wang, X. Z.; Liu, X. J.; Ying, Y. B. Wearable plasmonic-metasurface sensor for noninvasive and universal molecular fingerprint detection on biointerfaces. *Sci. Adv.* **2021**, *7*, e4553.

[207] He, X.; Zhou, X.; Liu, Y.; Wang, X. L. Ultrasensitive, recyclable and portable microfluidic surface-enhanced Raman scattering (SERS) biosensor for uranyl ions detection. *Sens. Actuators B:Chem.* **2020**, *311*, 127676.

[208] Jin, X. Y.; Guo, P. R.; Guan, P.; Wang, S.; Lei, Y. Q.; Wang, G. H. The fabrication of paper separation channel based SERS substrate and its recyclable separation and detection of pesticides. *Spectrochim. Acta Part A:Mol. Biomol. Spectrosc.* **2020**, *240*, 118561.

[209] Li, H. J.; Wang, M. C.; Shen, X. X.; Liu, S.; Wang, Y.; Li, Y.; Wang, Q. W.; Che, G. B. Rapid and sensitive detection of enrofloxacin hydrochloride based on surface enhanced Raman scattering-active flexible membrane assemblies of Ag nanoparticles. *J. Environ. Manage.* **2019**, *249*, 109387.

[210] Sun, H. M.; Li, X. T.; Hu, Z. Y.; Gu, C. J.; Chen, D.; Wang, J.; Li, B.; Jiang, T.; Zhou, X. F. Hydrophilic–hydrophobic silver nanowire-paper based SERS substrate for *in-situ* detection of furazolidone under various environments. *Appl. Surf. Sci.* **2021**, *556*, 149748.

[211] Salthammer, T.; Mentese, S.; Marutzky, R. Formaldehyde in the indoor environment. *Chem. Rev.* **2010**, *110*, 2536–2572.

[212] Sun, J. J.; Zhang, Z. Q.; Liu, C.; Dai, X. D.; Zhou, W. P.; Jiang, K. M.; Zhang, T.; Yin, J.; Gao, J.; Yin, H. C. et al. Continuous *in situ* portable SERS analysis of pollutants in water and air by a highly sensitive gold nanoparticle-decorated PVDF substrate. *Anal. Bioanal. Chem.* **2021**, *413*, 5469–5482.

[213] Li, L. M.; Chin, W. S. Rapid fabrication of a flexible and transparent Ag nanocubes@PDMS film as a SERS substrate with high performance. *ACS Appl. Mater. Interfaces* **2020**, *12*, 37538–37548.

[214] Zeisel, S. H.; Da Costa, K. A. Choline: An essential nutrient for public health. *Nutr. Rev.* **2009**, *67*, 615–623.

[215] Weng, G. J.; Feng, Y.; Zhao, J.; Li, J. J.; Zhu, J.; Zhao, J. W. Sensitive detection of choline in infant formulas by SERS marker transformation occurring on a filter-based flexible substrate. *Sens. Actuators B:Chem.* **2020**, *308*, 127754.

[216] Li, Z. B.; Meng, G. W.; Huang, Q.; Hu, X. Y.; He, X.; Tang, H. B.; Wang, Z. W.; Li, F. D. Ag nanoparticle-grafted PAN-nanohump array films with 3D high-density hot spots as flexible and reliable SERS substrates. *Small* **2015**, *11*, 5452–5459.

[217] Wu, J. J.; Feng, Y.; Zhang, L.; Wu, W. B. Nanocellulose-based surface-enhanced Raman spectroscopy sensor for highly sensitive detection of TNT. *Carbohydr. Polym.* **2020**, *248*, 116766.

[218] Shi, Y. E.; Wang, W. S.; Zhan, J. H. A positively charged silver nanowire membrane for rapid on-site swabbing extraction and detection of trace inorganic explosives using a portable Raman spectrometer. *Nano Res.* **2016**, *9*, 2487–2497.

[219] Lussier, F.; Thibault, V.; Charron, B.; Wallace, G. Q.; Masson, J. F. Deep learning and artificial intelligence methods for Raman and surface-enhanced Raman scattering. *TrAC Trends Anal. Chem.* **2020**, *124*, 115796.

[220] Lussier, F.; Missirlis, D.; Spatz, J. P.; Masson, J. F. Machine-learning-driven surface-enhanced Raman scattering optophysiology reveals multiplexed metabolite gradients near cells. *ACS Nano* **2019**, *13*, 1403–1411.

[221] Huang, Z. F.; Siddhanta, S.; Zheng, G.; Kickler, T.; Barman, I. Rapid, label-free optical spectroscopy platform for diagnosis of heparin-induced thrombocytopenia. *Angew. Chem., Int. Ed.* **2020**, *59*, 5972–5978.

[222] Liu, X. B.; Zhang, Z. M.; Sousa, P. F. M.; Chen, C.; Ouyang, M. L.; Wei, Y. C.; Liang, Y. Z.; Chen, Y.; Zhang, C. P. Selective iteratively reweighted quantile regression for baseline correction. *Anal. Bioanal. Chem.* **2014**, *406*, 1985–1998.

[223] Steinier, J.; Termonia, Y.; Deltour, J. Smoothing and differentiation of data by simplified least square procedure. *Anal. Chem.* **1972**, *44*, 1906–1909.

[224] Xi, Y.; Li, Y. E.; Duan, Z. Z.; Lu, Y. A novel pre-processing algorithm based on the wavelet transform for Raman spectrum. *Appl. Spectrosc.* **2018**, *72*, 1752–1763.

[225] Feuerstein, D.; Parker, K. H.; Boutelle, M. G. Practical methods for noise removal: Applications to spikes, nonstationary quasi-periodic noise, and baseline drift. *Anal. Chem.* **2009**, *81*, 4987–4994.

[226] Eilers, P. H. C. A perfect smoother. *Anal. Chem.* **2003**, *75*, 3631–3636.

[227] Zhang, Z. M.; Chen, S.; Liang, Y. Z. Baseline correction using adaptive iteratively reweighted penalized least squares. *Analyst* **2010**, *135*, 1138–1146.

[228] Sattlecker, M.; Stone, N.; Bessant, C. Current trends in machine-learning methods applied to spectroscopic cancer diagnosis. *TrAC Trends Anal. Chem.* **2014**, *59*, 17–25.

[229] Shin, H.; Jeong, H.; Park, J.; Hong, S.; Choi, Y. Correlation between cancerous exosomes and protein markers based on surface-enhanced Raman spectroscopy (SERS) and principal component analysis (PCA). *ACS Sens.* **2018**, *3*, 2637–2643.

[230] Taylor, J. N.; Mochizuki, K.; Hashimoto, K.; Kumamoto, Y.; Harada, Y.; Fujita, K.; Komatsuzaki, T. High-resolution Raman microscopic detection of follicular thyroid cancer cells with unsupervised machine learning. *J. Phys. Chem. B* **2019**, *123*, 4358–4372.

[231] Lim, J. Y.; Nam, J. S.; Shin, H.; Park, J.; Song, H. I.; Kang, M.; Lim, K. I.; Choi, Y. Identification of newly emerging influenza viruses by detecting the virally infected cells based on surface enhanced Raman spectroscopy and principal component analysis. *Anal. Chem.* **2019**, *91*, 5677–5684.

[232] Xie, L. P.; Li, Z. L.; Zhou, Y. H.; He, Y. L.; Zhu, J. X. Computational diagnostic techniques for electrocardiogram signal analysis. *Sensors* **2020**, *20*, 6318.

[233] Feng, S. Y.; Lin, D.; Lin, J. Q.; Li, B. H.; Huang, Z. F.; Chen, G. N.; Zhang, W.; Wang, L.; Pan, J. J.; Chen, R. et al. Blood plasma surface-enhanced Raman spectroscopy for non-invasive optical detection of cervical cancer. *Analyst* **2013**, *138*, 3967–3974.

[234] Szymańska, E.; Gerretzen, J.; Engel, J.; Geurts, B.; Blanchet, L.; Buydens, L. M. C. Chemometrics and qualitative analysis have a vibrant relationship. *TrAC Trends Anal. Chem.* **2015**, *69*, 34–51.

[235] Gromski, P. S.; Muhamadali, H.; Ellis, D. I.; Xu, Y.; Correa, E.; Turner, M. L.; Goodacre, R. A tutorial review: Metabolomics and partial least squares-discriminant analysis—A marriage of convenience or a shotgun wedding. *Anal. Chim. Acta* **2015**, *879*,

10–23.

[236] Li, S. X.; Zhang, Y. J.; Xu, J. F.; Li, L. F.; Zeng, Q. Y.; Lin, L.; Guo, Z. Y.; Liu, Z. M.; Xiong, H. L.; Liu, S. H. Noninvasive prostate cancer screening based on serum surface-enhanced Raman spectroscopy and support vector machine. *Appl. Phys. Lett.* **2014**, *105*, 091104.

[237] Shin, H.; Oh, S.; Hong, S.; Kang, M.; Kang, D.; Ji, Y. G.; Choi, B. H.; Kang, K. W.; Jeong, H.; Park, Y. et al. Early-stage lung cancer diagnosis by deep learning-based spectroscopic analysis of circulating exosomes. *ACS Nano* **2020**, *14*, 5435–5444.

[238] Wani, J. A.; Sharma, S.; Muzamil, M.; Ahmed, S.; Sharma, S.; Singh, S. Machine learning and deep learning based computational techniques in automatic agricultural diseases detection: Methodologies, applications, and challenges. *Arch. Comput. Methods Eng.*, in press, http://doi.org.10.1007/s11831-021-09588-5.

[239] Liao, M. H.; Zheng, S. S.; Pan, S. X.; Lu, D. J.; He, W. Q.; Situ, G. H.; Peng, X. Deep-learning-based ciphertext-only attack on optical double random phase encryption. *Opto-Electron. Adv.* **2021**, *4*, 200016.

[240] Tadesse, L. F.; Safir, F.; Ho, C. S.; Hasbach, X.; Khuri-Yakub, B. P.; Jeffrey, S. S.; Saleh, A. A. E.; Dionne, J. Toward rapid infectious disease diagnosis with advances in surface-enhanced Raman spectroscopy. *J. Chem. Phys.* **2020**, *152*, 240902.

[241] Ho, C. S.; Jean, N.; Hogan, C. A.; Blackmon, L.; Jeffrey, S. S.; Holodniy, M.; Banaei, N.; Saleh, A. A. E.; Ermon, S.; Dionne, J. Rapid identification of pathogenic bacteria using Raman spectroscopy and deep learning. *Nat. Commun.* **2019**, *10*, 4927.

[242] Zhang, X. L.; Lin, T.; Xu, J. F.; Luo, X.; Ying, Y. B. DeepSpectra: An end-to-end deep learning approach for quantitative spectral analysis. *Anal. Chim. Acta* **2019**, *1058*, 48–57.

[243] Acquarelli, J.; Van Laarhoven, T.; Gerretzen, J.; Tran, T. N.; Buydens, L. M. C.; Marchiori, E. Convolutional neural networks for vibrational spectroscopic data analysis. *Anal. Chim. Acta* **2017**, *954*, 22–31.

[244] Erzina, M.; Trelin, A.; Guselnikova, O.; Dvorankova, B.; Strnadova, K.; Perminova, A.; Ulbrich, P.; Mares, D.; Jerabek, V.; Elashnikov, R. et al. Precise cancer detection via the combination of functionalized SERS surfaces and convolutional neural network with independent inputs. *Sens. Actuators B:Chem.* **2020**, *308*, 127660.

[245] Tran, V.; Walkenfort, B.; König, M.; Salehi, M.; Schlücker, S. Rapid, quantitative, and ultrasensitive point-of-care testing: A portable SERS reader for lateral flow assays in clinical chemistry. *Angew. Chem., Int. Ed.* **2019**, *58*, 442–446.